

# Randomized Gradient Descents on Riemannian Manifolds: Almost Sure Convergence to Global Minima in and beyond Quantum Optimization

Emanuel Malvetti<sup>1,2</sup>, Christian Arenz<sup>3</sup>, Gunther Dirr<sup>4</sup>,  
Thomas Schulte-Herbrüggen<sup>1,2</sup>

<sup>1</sup>School of Natural Sciences, Technische Universität München, Garching,  
85737, Germany.

<sup>2</sup>Munich Center for Quantum Science and Technology (MCQST) &  
Munich Quantum Valley (MQV), München, 80799, Germany.

<sup>3</sup>School of Electrical, Computer and Energy Engineering, Arizona State  
University, Tempe, 85287, Arizona, USA.

<sup>4</sup>Department of Mathematics, University of Würzburg, Würzburg,  
97074, Germany.

Contributing authors: [emanuel.malvetti@tum.de](mailto:emanuel.malvetti@tum.de);  
[christian.arenz@asu.edu](mailto:christian.arenz@asu.edu); [dirr@mathematik.uni-wuerzburg.de](mailto:dirr@mathematik.uni-wuerzburg.de);  
[tosh@tum.de](mailto:tosh@tum.de);

## Abstract

We analyze the convergence properties of gradient descent algorithms on Riemannian manifolds. We study randomization of the tangent space directions of Riemannian gradient flows for minimizing smooth cost functions (of Morse–Bott type) to obtain convergence to local optima. We prove that through randomly projecting Riemannian gradients according to the Haar measure, convergence to local optima can be obtained almost surely despite the existence of saddle points. As an application we consider ground state preparation through quantum optimization over the unitary group. In this setting one can efficiently approximate the Haar-random projections by implementing unitary 2-designs on quantum computers. We prove that the respective algorithm almost surely converges to the global minimum that corresponds to the ground state of a desired Hamiltonian. Finally, we discuss the time required by the algorithm to pass a saddle point in a simple two-dimensional setting.

**Keywords:** Riemannian gradient system, randomized gradient descent, Morse–Bott systems, saddle-point escape, quantum optimization

**MSC Classification:** 65K10 , 53B21 , 37H10

## 1 Introduction

Both gradient systems and numerical linear algebra come with a long history as well as a vibrant research activity. For instance, gradient systems have been advanced lately from Hilbert manifolds [Neuberger \(2010\)](#) to general metric spaces (e.g., in the context of optimal mass transport [Ambrosio et al \(2021\)](#); [Mielke \(2023\)](#)). In contrast, numerical linear algebra has faced factorization problems of huge tensor structures [Batselier et al \(2018\)](#) (tensor SVD) using “randomization strategies” for their classical algorithms in order to handle these amounts of data. Only a few decades ago a systematic study of their interplay started by analyzing the QR-algorithm and interior point methods from a (Riemannian) geometric point of view, cf. the collection of [Bloch \(1994\)](#). In this development the seminal work of [Brockett \(1988, 1989\)](#) on the so-called “double-bracket flow” on orbits of the orthogonal group (and likewise of the unitary group in [Brockett \(1993\)](#)), followed by independent similar ideas of [Chu and Driessel \(1990\)](#), has sparked a plethora of applications. For an early overview on optimization techniques on Riemannian manifolds (including higher-order methods) see [Smith \(1994\)](#) in [Bloch \(1994\)](#). A mathematical account in all detail can be found in the monograph by [Helmke and Moore \(1994\)](#) including discretization schemes, suitable step sizes, and proofs of convergence. For the latter, the authors heavily exploited the Morse-Bott structure of the cost function (i.e. the particular structure of the Hessian at possibly non-isolated critical points, cf. Subsec. 2.3 and [Duistermaat et al \(1983\)](#)) to obtain convergence to a single critical point. Based on these developments, higher-order methods with applications to further cost functions on classical matrix manifolds are treated in [Absil et al \(2008\)](#). In [Schulte-Herbrüggen et al \(2010\)](#) these ideas have been extended to flows and their discretization schemes on more general homogeneous spaces. There they were also connected to applications in quantum dynamics as well as to applications in numerical (multi-)linear algebra like higher-rank tensor approximations—as elaborated by [Curtef et al \(2012\)](#) to complement standard methods (like higher-order powers of [de Lathauwer et al \(2000\)](#) or quasi Newton methods of [Savas and Lim \(2010\)](#)).

Independently, in the physics community, [Wegner \(1994\)](#) (re)devised gradient flows of Brockett type, e.g., to (band-)diagonalize Hamiltonians, which the monograph by [Kehrein \(2006\)](#) elaborated to address further quantum many-body applications.

Often gradient-flow approaches for deriving optimization schemes on Riemannian manifolds hinge on the computability of the Riemannian exponential ensuring to take the gradient from the tangent space back on the manifold. To be precise, this is crucial whenever the manifold cannot be identified with its tangent spaces such as for the unitary group or unitary orbits.

With these stipulations, Riemannian optimization techniques constitute a versatile toolbox, since a cost function can readily be tailored to the particular application such as finding extremal eigen- or singular values (i.e. problems otherwise addressed by variational approaches). These instances also connect to other branches of mathematics such as numerical and  $C$ -numerical ranges and their extremal values, the numerical and  $C$ -numerical radii (see [Gustafson and Rao \(1997\)](#); [Li \(1994\)](#)).

Over the last decade, techniques from Riemannian optimization have also been adopted in quantum information science. For example, in quantum computing, hybrid quantum-classical algorithms [Bharti et al \(2022\)](#), such as variational quantum algorithms (VQAs) [Cerezo et al \(2021\)](#); [Tilly et al \(2022\)](#), have been developed to solve ground state problems [Peruzzo et al \(2014\)](#) (i.e. typically minimal eigenvalue problems), combinatorial optimization [Farhi et al \(2014\)](#), and quantum machine learning problems [Biamonte et al \(2017\)](#). In VQAs a fixed parameterized quantum circuit, i.e. a parameterized set of unitary transformations (usually implemented by a fixed set of unitary gates), is iteratively optimized in tandem with a classical computer to minimize a cost function whose global optima encode the solution(s) to the desired problem. More precisely, a quantum processor, including a measurement device, is used to output the current (e.g., expectation) value of the cost function in each iterative step. Interleaved, the classical computer component provides the optimization routine that determines the parameter update for the next iteration on the quantum processor. Since quantum computers can, in principle, handle some classically exponentially complex problems, the hope is that VQAs will be able to solve problems of large size a solely classical algorithm would be incapable of.

However, since the optimization problems VQAs aim to solve are typically non-convex, which can often be traced back to the quantum circuit parameterization [Magann et al \(2021\)](#); [Lee et al \(2021\)](#), the iterative search for the optimal parameters can get stuck in suboptimal solutions [Bittel and Kliesch \(2021\)](#).

To overcome this challenge, adaptive quantum algorithms have been designed. Instead of fixing a quantum circuit and picking a parameterization as in VQAs, adaptive algorithms successively grow a quantum circuit informed by measurement data from the quantum processor. In this approach the cost function is minimized *while* the quantum circuit is grown, see [Grimsley et al \(2019\)](#); [Wiersema and Killoran \(2023\)](#); [Magann et al \(2022, 2023\)](#). One of the most prominent examples of such a strategy is the so-called ADAPT-VQE algorithm [Grimsley et al \(2019\)](#), which was originally proposed to solve ground state problems in chemistry, and was further developed later to solve combinatorial optimization problems on quantum computers [Tang et al \(2021\)](#).

Unfortunately, since typically in adaptive quantum algorithms the circuit growth is informed by gradient estimates performed by the quantum computer, adaptive quantum algorithms face similar challenges as VQAs, i.e., the adaptive circuit growth can get stuck when gradients vanish. This issue has recently been addressed by identifying adaptive quantum algorithms as quantum computer implementations of Riemannian gradient flows on the special unitary group  $SU(d)$  of dimension  $d = 2^n$  where  $n$  is the number of qubits of the quantum computer [Wiersema and Killoran \(2023\)](#). Since implementing Riemannian gradient methods on quantum computers requires in general exponential resources (i.e., the number of gates and/or the number of iterations

of the corresponding quantum circuit grows exponentially in  $n$ ). [Wiersema and Kildoran \(2023\)](#) proposed projecting the Riemannian gradient into smaller dimensional subspaces that scale polynomially in  $n$ , which in turn yields scalable quantum computer implementations. However, the proposed “dimension reduction” strategy of the Riemannian gradient to obtain efficient quantum computer implementations comes with a cost: While it can be shown that in the quantum computing setting (i.e., the Riemannian gradient flow on the special unitary group for ground state problems) the full gradient flow converges almost surely to the problem solution given by the global minimizer, despite the existence of strict saddle points (i.e., saddle points at which the Hessian has at least one negative eigenvalue) [Lee et al \(2019\)](#), for the projected versions no convergence guarantees can be made. Indeed, numerical simulations suggest that existing versions of gradient algorithms that are efficiently implementable on quantum computers also suffer from converging to suboptimal solutions. Inspired by the success of classical randomized gradient descent [Ruder \(2016\)](#), this problem has most recently been addressed by some of the authors in [Magann et al \(2023\)](#) via “random projections” of the Riemannian gradient, as depicted in Fig. 1, which are efficiently implementable on quantum computers. An efficient quantum computer implementation of these random directions can be achieved through exact *and* approximate unitary 2-designs [Dankert et al \(2009\)](#). The numerical experiments presented in [Magann et al \(2023\)](#) indicate that such a randomization procedure of the Riemannian gradient indeed yields (almost surely) convergence to the problem solution.

In this paper we consider the randomized gradient algorithm presented in [Magann et al \(2023\)](#) in the more general setting of Morse–Bott cost functions on Riemannian manifolds. For both continuous and discrete probability distributions of the random gradient directions we prove that the algorithm almost surely converges to a local minimum even. Finally we show how the result can be applied to quantum optimization tasks, such as ground state preparation. In the quantum setting there are no local optima, thereby we prove that the randomized gradient algorithm converges almost surely to the global minimum.

## Structure and Main Results

In Sec. 2 we introduce the fundamental notions from Riemannian geometry to describe gradient flows (Sec. 2.1), recollecting some well-known results on the convergence of gradient flows (Sec. 2.2), and their algorithmic implementation as gradient descents (Sec. 2.4). In Sec. 3 we describe a gradient descent algorithm where in each step the full gradient of a high-dimensional problem is projected on just a randomly chosen direction of the tangent space, considering both continuous and discrete distributions.

The main main result is obtained in Secs. 3.2 and 3.3, where we prove that a randomly projected gradient descent algorithm to a smooth Morse–Bott function (with compact sublevel sets) on a Riemannian manifold comes with two vitally beneficial properties: (i) *it almost surely escapes saddle points*—as is shown in Lem. 3.11 and as a consequence (ii) *it almost surely converges a local minimum*—as shown in Thm. 3.14.

In Sec. 4 the case of a two-dimensional saddle point is studied approximately using analytical methods and also using numerical simulation. We obtain good approximations for the time necessary to pass the saddle point.

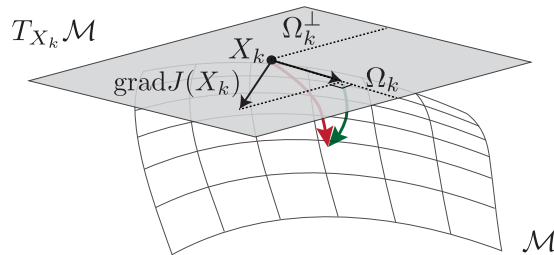


**Fig. 1** Schematic representation of the randomized gradient descent algorithm on a Riemannian manifold  $\mathcal{M}$ . At a point  $X_k$  on  $\mathcal{M}$  the Riemannian gradient  $\text{grad} J(X_k)$  of a cost function  $J : \mathcal{M} \rightarrow \mathbb{R}$  lies in the tangent space  $T_{X_k} \mathcal{M}$  depicted as plane spanned by  $\Omega_k$  and its orthocomplement  $\Omega_k^\perp$ . Instead of iteratively following the full gradient in order to optimize  $J$ , here in each step we consider a projection of  $\text{grad} J(X_k)$  onto a randomly chosen tangent-space direction  $\Omega_k$ . This is key for *efficient* implementations of gradient flows in large-scale quantum optimization problems. In the case of the special unitary group the randomized directions are given by (traceless) skew-Hermitian operators  $\Omega_k = iH_k$ . The corresponding quantum circuit consists of a sequence of unitary transformations as shown in Fig. 2.

Finally Sec. 5 shows how the previous results can be applied in quantum optimization to the problem of ground state preparation.

## 2 Riemannian Gradient Flow and Descent

### 2.1 Basic Concepts

First we recall some basic notions and notations from Riemannian geometry. Let  $M$  denote a finite dimensional smooth manifold of dimension  $n$  with tangent and cotangent bundles  $TM$  and  $T^*M$ , respectively. Moreover, let  $M$  be endowed with a Riemannian metric  $g$ , i.e. a smoothly varying scalar product  $g(\mathbf{x}) = \langle \cdot, \cdot \rangle_{\mathbf{x}}$  on each tangent space  $T_{\mathbf{x}}M$ ,  $\mathbf{x} \in M$ . The pair  $(M, g)$  is called a *Riemannian manifold*.

Every Riemannian manifold is equipped with a Riemannian density  $\mu$  induced by the metric  $g$ , see (Lee, 2013, Prop. 2.44). This density can be used to integrate functions, to induce a measure on  $M$  and to define sets of measure zero. Equivalently (but without introduction a Riemannian density), one could say that  $S \subset M$  has measure zero if there is an atlas such that  $S \cap \text{dom } \sigma$  has Lebesgue measure zero in every chart  $\sigma$ . In particular any submanifold of dimension strictly smaller than  $N$  has measure zero.

### 2.2 Gradient Flows and Asymptotic Behaviour (I)

In the following general description, we depart from the above notation of ‘the’ cost function  $J$  borrowed from quantum optimization and introduce  $f : M \rightarrow \mathbb{R}$  for an arbitrary smooth (cost) function on  $M$  with differential  $df : M \rightarrow T^*M$ . Then the gradient of  $f$  at  $\mathbf{x} \in M$ , denoted by  $\text{grad} f(\mathbf{x})$ , is the unique vector in  $T_{\mathbf{x}}M$  determined by the identity

$$df(\mathbf{x})\xi = \langle \text{grad} f(\mathbf{x}), \xi \rangle_{\mathbf{x}} \quad (1)$$

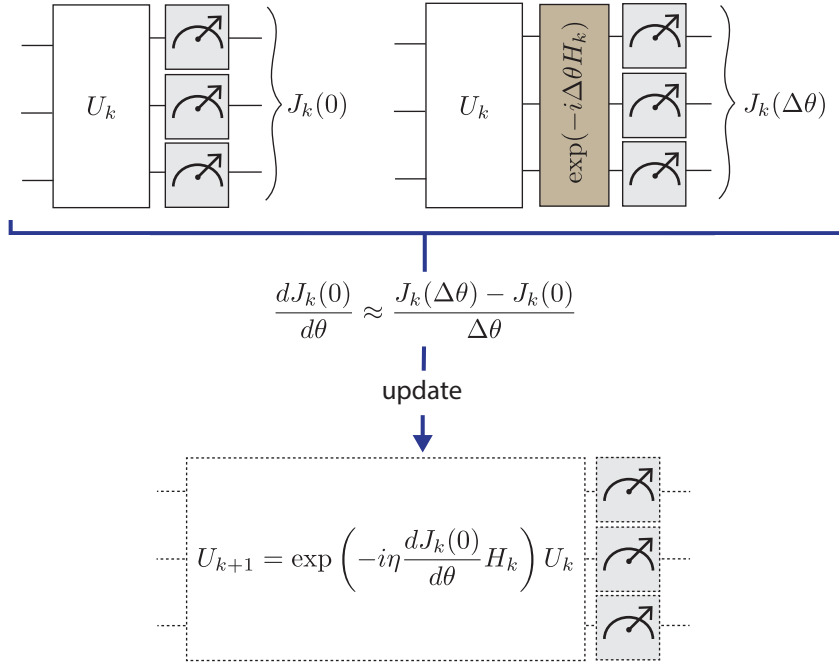


**Fig. 2** Schematic implementation of the discretized Riemannian gradient scheme by a quantum algorithm in case the manifold is  $\mathcal{M} = SU(2^n)$  or  $\mathcal{M} = Ad_{SU(2^n)}$ . For both instances the dimension of the problem scales exponentially with the number  $n$  of quantum particles (here qubits). Each quantum circuit  $U_k$  is adaptively turned into  $U_{k+1} = \exp\left(-i\eta \frac{dJ_k(0)}{d\theta} H_k\right) U_k$  by moving in a random tangent-space direction  $iH_k$  whose corresponding projection  $\frac{dJ_k(0)}{d\theta} = \langle \text{grad}J(U_k), iH_k U_k \rangle$  is measured on a quantum device, where  $\eta$  denotes the learning rate and we define the cost-function value at the  $k$ -th iteration as  $J_k(x) \equiv J(x, U_k)$  where  $J(x, U_k) = \text{tr}\{A \exp(-ixH_k) U_k \rho U_k^* \exp(ixH_k)\}$  (see Sec. 5). The measurement projection is done on the quantum computer, and the statistics of repeated measurements for the expectation value is done on the classical computer. In this way a randomized gradient flow as in Fig. 1 is implemented. In this work we show that for sufficiently small  $\eta$  such a (discretized) flow converges almost surely to the global optimum.

for all  $\xi \in T_{\mathbf{x}}M$ . Equation (1) naturally defines a vector field on  $M$  via  $\text{grad} f : M \rightarrow TM$ ,  $\mathbf{x} \rightarrow \text{grad} f(\mathbf{x})$  called gradient vector field of  $f$ . The corresponding ordinary differential equation

$$\dot{\mathbf{x}} = -\text{grad} f(\mathbf{x}) =: F(\mathbf{x}) \quad (2)$$

and its flow are referred to as the gradient system and the gradient flow of  $f$ , respectively.

In local coordinates the above reads as follows: Let  $\sigma : U \rightarrow \mathbb{R}^n$  be a chart about  $\mathbf{x} \in M$ , denote  $\mathbf{y} = \sigma(\mathbf{x})$ , and let  $\tilde{f} := f \circ \sigma^{-1}$  be the chart representation of  $f$ . Moreover let  $\tilde{g} := (\sigma^{-1})^* g$  be the chart representation of the metric  $g$  on  $\sigma(U)$ , i.e.  $\tilde{g}(\mathbf{y}) = \sum_{i,j=1}^n \tilde{g}_{ij}(\mathbf{y}) dy^i dy^j$ , where  $\tilde{G}(\mathbf{y}) := (\tilde{g}_{ij}(\mathbf{y}))$  is a positive definite matrix varying smoothly in  $\mathbf{y} \in \sigma(U)$ . Finally let  $\tilde{F} := (\sigma^{-1})^* F$  be the chart representation

of the gradient vector field  $\text{grad } f$ . Then it holds that

$$\tilde{F}^j(\mathbf{y}) = \sum_{i=1}^n \tilde{g}^{ij}(\mathbf{y}) \frac{\partial \tilde{f}}{\partial y_i}(\mathbf{y}),$$

where  $\tilde{g}^{ij}(\mathbf{y})$  are the entries of the inverse of  $\tilde{G}(\mathbf{y})$  and  $\frac{\partial}{\partial y_i}$  denotes the  $i$ -th partial derivative.

Any convergence analysis of gradient systems is based on the following two observations: (i) the critical points of  $f$  are the equilibria of (2), (ii)  $f$  constitutes a Lyapunov function for (2), i.e.  $f$  is monotonically decreasing along solutions. Despite their simplicity they immediately allow several non-trivial statements about the asymptotic behavior of (2) which can be characterized by its  $\omega$ -limit sets

$$\omega(\mathbf{x}_0) := \bigcap_{s>0} \overline{\{\varphi(t, \mathbf{x}_0) \mid t > s\}},$$

where  $t \mapsto \varphi(t, \mathbf{x}_0)$  denotes the unique solution of (2) with initial value  $\varphi(0, \mathbf{x}_0) = \mathbf{x}_0$ .

**Proposition 2.1** (Lee (2013)). *If  $f$  has compact sublevel sets, i.e. if the sets  $\{\mathbf{x} \in M : f(\mathbf{x}) \leq c\}$  are compact for all  $c \in \mathbb{R}$ , then every solution of (2) exists for  $t \geq 0$  and its  $\omega$ -limit set is a non-empty, compact and connected subset of the set of critical points of  $f$ .*

Although, Proposition 2.1 shows that  $\omega(\mathbf{x})$  is contained in the set of critical points of  $f$  it does not guarantee convergence to a single critical point and, indeed, there are smooth gradient systems the trajectories of which exhibit a non-trivial convergence behavior to the set of critical points (cf. ‘‘Mexican hat counter-example’’ by Curry (1944)). Yet for isolated critical points one has the following trivial consequence of Proposition 2.1.

**Corollary 2.2.** *If  $f$  has compact sublevel sets and all critical points are isolated, then any solution of (2) converges (for  $t \rightarrow \infty$ ) to a single critical point of  $f$ . Moreover if additionally all saddle points are strict<sup>1</sup> then for almost all initial points (in the sense of Sec. 2.1) the flow converges to a local minimum.*

Continua of critical points are much more subtle to handle. Some enhanced conditions guaranteeing convergence to a single critical point will be briefly discussed in the next subsection.

### 2.3 The Hessian, Morse–Bott Functions and Asymptotic Behaviour (II)

As in the Euclidian case, linearizing the vector field  $F$  at its equilibria sheds light on its local stability. Clearly, since  $F = \text{grad } f$  constitutes a gradient vector field, its linearization at an equilibrium  $\mathbf{x} \in M$  is given by the Hessian  $H_f(\mathbf{x})$  of  $f$  at  $\mathbf{x} \in M$ . In

---

<sup>1</sup>see Subsec. 2.3 below

general, if  $M$  is non-Euclidian, the computation of  $H_f(\mathbf{x})$  can be rather involved. Yet, at critical points  $\mathbf{x}_0 \in M$  of  $f$ , the *Hessian* is given by the symmetric bilinear form

$$H_f(\mathbf{x}_0)(\xi, \eta) := \sum_{i,j=1}^n \tilde{H}(f \circ \sigma^{-1})(\sigma(\mathbf{x}_0))_{ij} (D\sigma(\mathbf{x}_0)\xi)_i (D\sigma(\mathbf{x}_0)\eta)_j, \quad (3)$$

where  $\sigma$  is any chart around  $\mathbf{x}_0 \in M$  and  $\tilde{H}(f \circ \sigma^{-1})$  denotes the ordinary Hesse matrix of the chart representation  $f \circ \sigma^{-1}$ . It is straightforward to show that (3) is independent of  $\sigma$ . Moreover, we will call  $\mathbf{x}_0$  a *strict saddle point* if  $H_f(\mathbf{x}_0)$  (or more precisely the associated symmetric operator) has at least one negative eigenvalue.

The above concepts allow a trivial generalization of a well-known result from elementary calculus which follows straightforwardly in local coordinates.

**Proposition 2.3.** *Let  $(M, g)$  be a Riemannian manifold and let  $\mathbf{x}$  be a critical point of  $f : M \rightarrow \mathbb{R}$ . If  $H_f(\mathbf{x})$  is positive definite, then  $\mathbf{x}$  is a strict local minimum of  $f$ .*

Now the question arises whether the (asymptotic) stability of an equilibrium  $\mathbf{x} \in M$  of (2) may depend on the Riemannian metric  $g$  — and the answer is surprisingly “yes”, cf. Takens (1971). However, certain properties such as being a strict local minimum or an isolated critical point are obviously not up to the choice of the metric, and thus the (asymptotic) stability of those equilibria is independent of the Riemannian metric as the next theorem shows.

**Theorem 2.4.** (a) *Every strict local minimum of  $f$  is a stable equilibrium of (2).*  
 (b) *Every strict local minimum of  $f$  which is additionally an isolated critical point is an asymptotically stable equilibrium of (2).*

Both assertions follow immediately from classical stability theory by taking  $f$  as Lyapunov function, cf. Helmke and Moore (1994); Irwin (1980). Handling non-isolated critical points is much more subtle. A first hint on how to approach this issue is obtained by Corollary 2.2 which could be restated (in a slightly weaker version) as follows:

*For Morse functions with compact sublevel sets every solution of the corresponding gradient system converges (for  $t \rightarrow \infty$ ) to a single critical point.*

This suggests to work with Morse–Bott functions when it comes to non-isolated critical point. Recall that a smooth function  $f : M \rightarrow \mathbb{R}$  is called *Morse–Bott function*, when the set  $C$  of critical points is a closed submanifold of  $M$  such that the tangent space of  $T_{\mathbf{x}}C$  coincides with the kernel of the Hessian operator for all  $\mathbf{x} \in C$ . Note that  $C$  is allowed to have several connected components with possibly different dimensions, (Helmke and Moore, 1994, p. 366), (Nicolaescu, 2011, Def. 2.41) or Banyaga and Hurtubise (2010). Thus Morse functions are particular Morse–Bott functions, where  $C$  consists of 0-dimensional manifolds (i.e. isolated points).

Now, the above concept allows a generalization of the Morse–Palais Lemma to Morse–Bott functions which is often called Morse–Bott Lemma, see Banyaga and Hurtubise (2004). It yields a local normal form of Morse–Bott functions near their critical



points, which reads in local coordinates as follows

$$\tilde{f}(\mathbf{x}, \mathbf{y}, \mathbf{z}) = \|\mathbf{x}\|^2 - \|\mathbf{y}\|^2,$$

with  $\mathbf{x} \in \mathbb{R}^{n_+}$ ,  $\mathbf{y} \in \mathbb{R}^{n_-}$ , and  $\mathbf{z} \in \mathbb{R}^{n_0}$ , where  $n_+$ ,  $n_-$  and  $n_0$  are the number of positive, negative and zero eigenvalues of the Hessian operator. This finally allows to prove that solutions of the respective gradient systems convergence to a single critical point.

**Theorem 2.5.** *Let  $f : M \rightarrow \mathbb{R}$  be a Morse–Bott function on a Riemannian manifold  $(M, g)$  with compact sublevel sets. Then every solution of the gradient flow (2) converges to a single critical point. Moreover for almost every initial point the flow converges to a local minimum.*

Finally, we recall another very powerful result for analyzing the convergence of gradient systems which is based on Lojasiewicz’s celebrated gradient estimate [Lojasiewicz \(1984\)](#). Let  $f : M \rightarrow \mathbb{R}$  be real analytic,  $\mathbf{x}_0 \in M$  a critical point of  $f$  and assume w.l.o.g.  $f(\mathbf{x}_0) = 0$ . Then near  $\mathbf{x}_0 \in M$  one has the estimate

$$\|\text{grad}(\mu \circ f)(\mathbf{x})\|_{\mathbf{x}} \geq c, \quad (4)$$

where  $\mu : \mathbb{R}^+ \rightarrow \mathbb{R}^+$  is a strictly increasing  $C^1$ -function and  $c > 0$  some positive constant, cf. ([Lageman, 2007](#), Cor. 1.1.25). In the literature, one usually find  $\mu(r) := r^{1-\theta}$  with  $\theta \in (0, 1)$ . Eq. (4) easily allows to bound the length of any trajectory of (2) whose  $\omega$ -limit set is non-empty. Hence one gets the following result.

**Theorem 2.6.** *Lojasiewicz (1984). Let  $(M, g)$  and  $f : M \rightarrow \mathbb{R}$  be real analytic. Then every non-empty  $\omega$ -limit set of (2) consists only of a single critical point.*

## 2.4 The Exponential Map and Numerical Gradient Descent

Finally, we approach the problem of discretization of (2) resulting in a convergent gradient descent method. The ideas presented here can be traced back to [Brockett \(1988, 1989\)](#) and [Smith \(1993, 1994\)](#). Let

$$\exp_{\mathbf{x}} : T_{\mathbf{x}}M \rightarrow M \quad (5)$$

denote the *Riemannian exponential map* at  $\mathbf{x} \in M$ , i.e.  $t \rightarrow \exp_{\mathbf{x}}(t\xi)$  is the unique geodesic with initial value  $\mathbf{x} \in M$  and initial velocity  $\xi \in T_{\mathbf{x}}M$ . Here, we assume for simplicity that  $(M, g)$  is (geodesically) complete, i.e. (5) is well-defined for the entire tangent space  $T_{\mathbf{x}}M$ . Probably the simplest discretization scheme given by

$$\mathbf{x}_{k+1} := \exp_{\mathbf{x}_k}(-\eta_k \text{grad} f(\mathbf{x}_k)), \quad (6)$$

can be seen as a “natural” generalization of the explicit Euler method. Here  $\eta_k > 0$  denotes an appropriate “step size”<sup>2</sup> which may depend on  $k \in \mathbb{N}$ .

---

<sup>2</sup>Note that the “actual” step size results from the modulus of  $\eta \text{grad} f(\mathbf{x}_k)$ .

In order to guarantee convergence of (6) to the set of critical points, it is sufficient to apply the Armijo rule, see [Luenberger and Ye \(2008\)](#). An alternative to Armijo’s rule provides the step-size selection suggested by [Brockett \(1993\)](#), see also [Helmke and Moore \(1994\)](#). Moreover, for compact Riemannian manifolds even a sufficiently small constant step size  $\eta > 0$  guarantees convergence:

**Theorem 2.7.** *For compact Riemannian manifolds every trajectory of the discretized gradient descent (6) (with constant but small enough step size) converges to the set of critical points. Moreover, the set of initial points converging to strict saddle points has measure zero—in the sense of [Sec. 2.1](#) here.*

The second part of the above statement can be found in ([Lee et al, 2019](#), Cor. 6)<sup>3</sup> Thus, for a function with compact sublevel sets, gradient descent (6) behaves similar as its continuous counter-part, cf. [Cor. 2.2](#), i.e. it converges almost surely to a local minimum if the step size is chosen small enough.

Deeper results which yield convergence to a single critical point are more subtle to derive. Here we present one result in this direction which is again based on the analyticity of the cost function  $f$  and on Łojasiewicz’s inequality.

**Theorem 2.8.** *[Lageman \(2007\)](#) If  $(M, g)$  and  $f$  are real analytic, and the step sizes are chosen according to a version of the first Wolfe–Powell condition for Riemannian manifolds, then pointwise convergence holds.*

**Remark 2.9.** *It should be mentioned that gradient descent algorithms are usually studied as exact algorithms, not as numerical algorithms where real numbers are represented as floating point values and arithmetic is not exact. Numerical effects can be important, for instance cancellation effects from computing gradients in a naive way. Nevertheless, this paper will ignore these numerical issues.*

Finally, in order to determine the largest admissible step size of our algorithm we need a notion of Lipschitz continuity of vector fields on Riemannian manifolds. Care has to be taken here since tangent vectors in different tangent spaces cannot be compared by default. Certainly, one can define local Lipschitz continuity via local charts but this does not allow to assign a meaningful Lipschitz constant to the vector field. A natural and intrinsic way to do this is to define Lipschitz continuity via parallel transport along the unique connecting geodesic, as is done in [Fetecau and Patacchini \(2022\)](#). Here, we use the following equivalent approach via Riemannian normal coordinates which result from any orthogonal coordinate system on  $T_{\mathbf{x}}M$  in combination with the Riemannian exponential map  $\exp_{\mathbf{x}}$ .

**Definition 1.** *Let  $(M, g)$  be a Riemannian manifold and let  $f : M \rightarrow \mathbb{R}$  be a smooth function. We say that  $f$  is  $\ell$ -smooth around  $\mathbf{x} \in M$  if there exist normal coordinates  $\tilde{f}$  around  $\mathbf{x}$  in which  $\nabla \tilde{f}$  is  $\ell$ -Lipschitz.*

---

<sup>3</sup>There the authors consider Riemannian manifolds embedded in the Euclidean space and retractions instead of an intrinsic Riemannian exponential function, but this does not restrict the generality of the result, cf. the Nash embedding theorem ([Berger, 2003](#), Thm. 46).

### 3 Algorithm and Convergence

We will study the following randomly projected gradient descent algorithm. Given a Riemannian manifold  $M$  of dimension  $N$ , a smooth function  $f : M \rightarrow \mathbb{R}$ , and a step size  $\eta > 0$  (with upper bound to be determined), the update rule is given by

$$\mathbf{x}_{i+1} = \exp_{\mathbf{x}_i}(-\eta g(\mathbf{x}_i, \mathbf{u}_i)), \quad g(\mathbf{x}, \mathbf{u}) = \langle \mathbf{u}, \text{grad } f(\mathbf{x}) \rangle \mathbf{u}, \quad \mathbf{S}_{\mathbf{x}_i}M \ni \mathbf{u}_i \stackrel{\text{i.i.d.}}{\sim} \mathcal{P}(\mathbf{x}_i), \quad (7)$$

where  $\mathbf{S}_{\mathbf{x}}M$  denotes the unit sphere in the tangent space  $\mathbb{T}_{\mathbf{x}}M$  and  $\mathcal{P}(\mathbf{x}_i)$  some probability measure on the unit sphere  $\mathbf{S}_{\mathbf{x}_i}M$ . Intuitively, the gradient is projected onto a randomly chosen direction  $\mathbf{u}$  at each step. Throughout we will consider two cases.

- Either  $\mathcal{P}(\mathbf{x}_i) = \mathcal{U}(\mathbf{S}_{\mathbf{x}_i}M)$  denotes the uniform (rotation invariant) probability distribution on the unit sphere, also called Haar measure;
- or  $\mathcal{P}(\mathbf{x}_i) = \mathcal{D}(\mathbf{S}_{\mathbf{x}_i}M)$  denotes a finite probability distribution on the unit sphere in some sense approximating a uniform distribution.

Let us clarify the case of a finite probability distribution. In this case we have  $k$  continuous vector fields  $\xi_j$  on  $M$  and continuous weights  $p_j : M \rightarrow \mathbb{R}$  with  $p_j > 0$  and  $\sum_{j=1}^k p_j \equiv 1$ . Then  $\mathbf{u}_i$  takes value  $\xi_j(\mathbf{x}_i)$  with probability  $p_j(\mathbf{x}_i)$ . Moreover we assume that at every point  $\mathbf{x}$ , the tangent vectors  $\xi_1(\mathbf{x}), \dots, \xi_k(\mathbf{x})$  span the entire tangent space even after removing all vectors collinear with some given direction  $\xi_j(\mathbf{x})$ .

Our goal is to analyze the convergence behaviour of this algorithm, and in particular to show that it converges almost surely to a local minimum of  $f$ . A deterministic version of the above described algorithm was analysed in (Absil et al, 2008, Def. 4.2.1, Thm. 4.3.1) under the heading “gradient-related methods”.

#### 3.1 Basic Properties

We start with some simple properties of the function  $g$  defined in (7).

**Lemma 3.1.** *Let  $\mathbf{x} \in M$  be given. If  $\mathbf{u} \in \mathbf{S}_{\mathbf{x}}M$ , then it holds that*

$$\langle \text{grad } f(\mathbf{x}), g(\mathbf{x}, \mathbf{u}) \rangle = \|g(\mathbf{x}, \mathbf{u})\|^2.$$

*Proof.* Using the definition of  $g(\mathbf{x}, \mathbf{u})$  and the fact that  $\mathbf{u}$  is a unit vector we immediately obtain  $\langle \text{grad } f(\mathbf{x}), g(\mathbf{x}, \mathbf{u}) \rangle = \langle \mathbf{u}, \text{grad } f(\mathbf{x}) \rangle^2 = \|g(\mathbf{x}, \mathbf{u})\|^2$ .  $\square$

Note that if  $\mathbf{u}$  is uniformly distributed on the sphere, then

$$\langle \mathbf{u}, \text{grad } f(\mathbf{x}) \rangle^2 \stackrel{d}{=} \mathbf{u}_N^2 \|\text{grad } f(\mathbf{x})\|^2,$$

where  $\stackrel{d}{=}$  means that the random variables have the same distribution.

**Remark 3.2.** *The image of the function  $u \mapsto g(\mathbf{x}, \mathbf{u})$  is a hypersphere in  $\mathbb{T}_{\mathbf{x}}M$  with center  $\frac{1}{2} \text{grad } f(\mathbf{x})$  and containing the origin. Let  $\mathbf{x} \in M$  be fixed and consider the map  $g_{\mathbf{x}} : \mathbf{S}_{\mathbf{x}}M \rightarrow \mathbb{T}_{\mathbf{x}}M$  given by  $\mathbf{u} \mapsto g(\mathbf{x}, \mathbf{u})$ . To simplify formulas, we choose an*

orthonormal basis  $(e_1, \dots, e_N)$  in  $\mathbb{T}_{\mathbf{x}}M$  such that  $\text{grad } f(\mathbf{x}) = \|\text{grad } f(\mathbf{x})\|e_N$ . In these coordinates the map  $g_{\mathbf{x}}$  is given by

$$g_{\mathbf{x}}(u_1, \dots, u_N) = u_N \|\text{grad } f(\mathbf{x})\| (u_1, \dots, u_N).$$

A straightforward computation shows that  $\|(u_N u_1, \dots, u_N^2 - \frac{1}{2})\| = \frac{1}{2}$ , and so the image of  $g_{\mathbf{x}}$  lies on a sphere with center  $\frac{1}{2} \text{grad } f(\mathbf{x})$  and passing through the origin. This induces a probability measure on the image. Consider the function

$$\tilde{g}(\mathbf{x}, \mathbf{v}) = \frac{1}{2}(\text{grad } f(\mathbf{x}) + \mathbf{v} \|\text{grad } f(\mathbf{x})\|),$$

and let  $v$  be distributed on the unit sphere according to a probability measure  $\mathcal{V}(\mathbb{S}_x M)$  such that  $g$  and  $\tilde{g}$  induce the same probability measure. The measure  $\mathcal{V}$  is not uniform on the sphere, but it is still invariant under rotations preserving  $\text{grad } f(\mathbf{x})$ . We see that  $v_N \sim 2u_N^2 - 1$ .

Note that since the standard deviation of  $u_N^2$  is larger than the expected value, Chebyshev's inequality cannot be applied to obtain useful concentration bounds. We will use a different method in Lemma A.2.

**Corollary 3.3.** *If  $\mathbb{E}[\mathbf{u}\mathbf{u}^\top] = \mathbf{1}/N$ , which is satisfied for the Haar measure, then it holds that*

$$\mathbb{E}[g(\mathbf{x}, \mathbf{u})] = \frac{\text{grad } f(\mathbf{x})}{N}$$

for any  $\mathbf{x} \in M$ .

*Proof.* This is a simple computation:  $\mathbb{E}[g(\mathbf{x}, \mathbf{u})] = \mathbb{E}[\mathbf{u}\mathbf{u}^\top \text{grad } f(\mathbf{x})] = \frac{1}{N} \text{grad } f(\mathbf{x})$ .  $\square$

The corollary shows that in this case the projected gradient is of size  $\text{grad } f(\mathbf{x})/N$ , and hence it is rather small for large  $N$ . Intuitively this happens because in high dimensions, a uniformly random unit vector  $u$  will be close to orthogonal to the gradient with high probability—after all, there are  $N - 1$  dimensions which are orthogonal to the gradient.

For large dimension  $N$  there exist good approximations of these distributions. In fact, the distribution of a coordinate of a uniformly random unit vector approximately follows a normal distribution, and hence its square approximates a  $\chi_1^2$  distribution. See Lemma A.2 for a precise result.

Now that we better understand the iteration rule, we want to understand by what amount the objective function value is likely to decrease after a certain number of iterations. It will be useful to use normal coordinate charts at the current point  $\mathbf{x}_i$ . These charts satisfy that the metric at the origin is trivial, and that geodesics passing through the origin are straight and uniformly parametrized, see for instance (Lee, 2013, Prop. 5.24). In particular, when using a normal coordinate chart about  $\mathbf{x}_i$ , the random variable  $\mathbf{x}_{i+1}$ , conditioned on  $\mathbf{x}_i$ , is still distributed on a hypersphere.

**Lemma 3.4.** *Let  $(M, g)$  be compact and let  $f : M \rightarrow \mathbb{R}$  be  $\ell$ -smooth at  $\mathbf{x}_i$  and with injectivity radius  $\text{inj}_M(\mathbf{x}_i)$ . Then for  $\eta \leq \min(1/\ell, \text{inj}_M(\mathbf{x}_i))$  it holds that*

$$f(\mathbf{x}_{i+1}) - f(\mathbf{x}_i) \leq -\eta \left(1 - \frac{\ell\eta}{2}\right) \langle \text{grad } f(\mathbf{x}_i), g(\mathbf{x}_i, \mathbf{u}_i) \rangle \leq 0.$$

*In particular the function value cannot increase.*

*Proof.* We choose a normal coordinate chart about  $\mathbf{x}_i$  and denote the coordinates by  $\tilde{\mathbf{x}}$  and the function in coordinates by  $\tilde{f}$ . In particular  $\tilde{\mathbf{x}}_i = 0$ . We may and do assume that  $\nabla \tilde{f}$  is  $\ell$ -Lipschitz. Note that at the origin  $\text{grad } \tilde{f}(\mathbf{x}_i) = \nabla \tilde{f}(\tilde{\mathbf{x}}_i)$  and the coordinate representation of  $\mathbf{x}_{i+1} = \exp_{\mathbf{x}_i}(-\eta g(\mathbf{x}_i, \mathbf{u}_i))$  is given by  $\tilde{\mathbf{x}}_{i+1} = -\eta g(\mathbf{x}_i, \mathbf{u}_i)$ . Then by (Nesterov, 2004, Lemma 1.2.3) and Lemma 3.1 it holds that

$$\begin{aligned} f(\mathbf{x}_{i+1}) - f(\mathbf{x}_i) &= \tilde{f}(\tilde{\mathbf{x}}_{i+1}) - \tilde{f}(\tilde{\mathbf{x}}_i) \\ &\leq \langle \nabla \tilde{f}(\tilde{\mathbf{x}}_i), \tilde{\mathbf{x}}_{i+1} - \tilde{\mathbf{x}}_i \rangle + \frac{\ell}{2} \|\tilde{\mathbf{x}}_{i+1} - \tilde{\mathbf{x}}_i\|^2 \\ &\leq -\eta \langle \text{grad } f(\mathbf{x}_i), g(\mathbf{x}_i, \mathbf{u}_i) \rangle + \frac{\ell\eta^2}{2} \|g(\mathbf{x}_i, \mathbf{u}_i)\|^2 \\ &= -\eta \left(1 - \frac{\ell\eta}{2}\right) \langle \text{grad } f(\mathbf{x}_i), g(\mathbf{x}_i, \mathbf{u}_i) \rangle, \end{aligned}$$

as desired. □

This result shows that, under the assumptions of Corollary 3.3, we obtain

$$\mathbb{E}[f(\mathbf{x}_{i+1}) - f(\mathbf{x}_i)] \leq -\frac{\eta}{N} \left(1 - \frac{\ell\eta}{2}\right) \|\text{grad } f(\mathbf{x}_i)\|^2.$$

More generally the previous result shows that the only way for the algorithm to stop improving is for the gradient to vanish:  $\text{grad } f(\mathbf{x}_i) \rightarrow 0$ .

**Corollary 3.5.** *If  $f(\mathbf{x}_i) \rightarrow c$  then  $c$  is a critical value and  $\mathbf{x}_i$  converges almost surely to the critical set of  $c$ .*

*Proof.* We will show that  $\Pr(f(\mathbf{x}_{i+1}) - f(\mathbf{x}_i) \rightarrow 0 \wedge \text{grad } f(\mathbf{x}_i) \not\rightarrow 0) = 0$ , which immediately implies that if the values  $f(\mathbf{x}_i)$  converge, then the gradients  $\text{grad } f(\mathbf{x}_i)$  converge to 0 almost surely. Note that if  $\text{grad } f(\mathbf{x}_i) \not\rightarrow 0$ , then there is some  $\varepsilon > 0$  such that  $\|\text{grad } f(\mathbf{x}_i)\| > \varepsilon$  on some infinite subsequence. Consider the case of the Haar measure. By the above, if  $f(\mathbf{x}_{i+1}) - f(\mathbf{x}_i) \rightarrow 0$ , then  $u_N^{(i)} \rightarrow 0$  on the same subsequence. Since the  $u_N^{(i)}$  are i.i.d (see Lemma A.1) and independent of the  $\mathbf{x}_i$  the probability that this happens is 0, and this concludes the proof. The case of discrete probability distributions follows immediately from Lemma A.3. □

## 3.2 Escaping Saddle Points

The main difficulty in proving almost sure convergence of the randomly projected gradient descent algorithm is to show that it does not get stuck in a saddle point.

Recall from Lemma 3.4 that the function value cannot increase. Hence, once we reach the critical value corresponding to some saddle point, without sitting in the saddle point itself, we say that we have “passed” the saddle point as now it is impossible to converge to the saddle point in question.

We start by proving the result in a simplified “isotropic” case, before treating the general case as a perturbation.

**Lemma 3.6.** *Consider the function  $f : \mathbb{R}^n \rightarrow \mathbb{R}$  defined by*

$$f(x_1, \dots, x_p, y_1, \dots, y_q, z_1, \dots, z_{n-p-q}) = a_1 x_1^2 + \dots + a_p x_p^2 - (b_1 y_1^2 + \dots + b_q y_q^2),$$

with  $1 \leq p, q$  and  $p + q \leq n$  as well as  $a_i, b_j > 0$ . Then  $f$  is  $\ell$ -smooth with  $\ell = 2 \max_{i,j}(a_i, b_j)$ . Moreover let  $0 < \eta \leq \frac{1}{\ell}$  and

$$\theta = \arctan\left(\frac{b_1 y_1^2 + \dots + b_q y_q^2}{a_1 x_1^2 + \dots + a_p x_p^2}\right) \in [0, \frac{\pi}{2}]. \quad (8)$$

Then there exist constants  $\varepsilon, \delta > 0$  such that for all<sup>4</sup>  $\theta \in [0, \frac{\pi}{3}]$  it holds that

$$\Pr(\theta_{i+1} - \theta_i \geq \varepsilon) \geq \delta.$$

*Proof.* The negative gradient of  $f$  is

$$\begin{aligned} -\nabla f(x_1, \dots, x_p, y_1, \dots, y_q, z_1, \dots, z_{n-p-q}) \\ = -2(a_1 x_1, \dots, a_p x_p, -b_1 y_1, \dots, -b_q y_q, 0, \dots, 0) \end{aligned}$$

and the value of  $\ell$  follows immediately. A key property of this simplified setting is that the gradient is a linear vector field on  $\mathbb{R}^n$ , and so the entire situation is invariant under scaling. From the definition of  $\theta$  it is clear that  $f$  vanishes if and only if  $\theta = \frac{\pi}{4}$ .

First note that due to the scaling invariance of the algorithm and of (8), we may focus on an initial point  $\mathbf{x}_i$  on the unit sphere  $S^{n-1}$ . After executing one step, we obtain a random improvement of our angle, namely  $\theta_{i+1} - \theta_i$  which depends on  $\mathbf{u}_i$  appearing in the update rule. Considering this improvement as a function of  $\mathbf{x}_i$  and  $\mathbf{u}_i$ , i.e.,

$$h(\mathbf{x}_i, \mathbf{u}_i) := \theta_i - \theta_i,$$

is clear that it is a continuous function. The optimal improvement achievable for a given  $\mathbf{x}_i$  is found by maximizing over  $\mathbf{u}_i$ . One can show that the resulting function is still continuous in  $\mathbf{x}_i$ . Moreover we claim that it is strictly positive on the sphere. Indeed, if  $\theta_i > 0$ , then this follows from the choice of  $\eta$ . If we perform a single (deterministic) negative gradient step with step size  $\eta$ , none of the coordinates will change sign, and whenever  $\theta \in (0, \frac{\pi}{2})$  its value will strictly increase. If  $\theta_i = 0$ , it is clear that the value of  $\theta$  will almost surely strictly increase, as the set of points  $\mathbf{x}_{i+1}$  with  $\theta_{i+1} = 0$  form a strict subspace of  $\mathbb{R}^n$ . Taken together this shows that there is some  $\varepsilon > 0$  such that the optimal improvement is at least  $2\varepsilon$  for every initial  $\mathbf{x}_{i+1}$ .

---

<sup>4</sup>The value  $\frac{\pi}{3}$  is arbitrary and could be replaced by any other value in  $(0, \frac{\pi}{2})$  without changing the proof.

It follows that for any given initial state  $\mathbf{x}_{i+1}$ , the probability that  $\theta_{i+1} - \theta_i \geq \varepsilon$  is strictly positive. Indeed,  $\mathbf{x}_{i+1}$  takes values on a sphere, and  $\theta(\cdot)$  is a continuous function on this sphere. The preimage of  $(\varepsilon, +\infty)$  on the sphere is a non-empty open set and hence has a strictly positive probability. Moreover one can show that this probability depends continuously on the initial state  $\mathbf{x}_i$ , and again we obtain a positive minimum  $\delta$  on the sphere by compactness. This proves that  $\Pr(\theta_{i+1} - \theta_i \geq \varepsilon) \geq \delta$  independently of the initial state.

Now consider the discrete case. Again we need to prove that there exist constants  $\varepsilon, \delta > 0$  such that for all  $\theta \in [0, \frac{\pi}{3}]$  it holds that  $\Pr(\theta_{i+1} - \theta_i \geq \varepsilon) \geq \delta$ .

The only cases where  $h(\mathbf{x}, \mathbf{u}) = 0$  (note that it cannot be negative) with probability one is when all  $v_j(\mathbf{x})$  for  $j = 1, \dots, k$  are either orthogonal to  $\text{grad}(\mathbf{x})$  or collinear to  $\mathbf{x}$ . By assumption, this cannot happen. Hence  $\max_j h(\mathbf{x}, \mathbf{v}_j)$  is non-negative and continuous, and on the compact set  $\{\mathbf{x} \in S^{n-1} : \theta(\mathbf{x}) \leq \pi/3\}$  it is even strictly positive. If we denote the minimum by  $\varepsilon$  and  $\delta = \frac{1}{k}$ , then the result follows.  $\square$

**Corollary 3.7.** *In the same setting as above, there exist  $\varepsilon, \delta > 0$  such that, with  $N = \lceil \frac{\pi}{3\varepsilon} \rceil$ , we have that*

$$\Pr(\theta_N \geq \frac{\pi}{3}) \geq \delta^N.$$

*It follows that for any  $m \in \mathbb{N}$*

$$\Pr(\theta_{mN} < \frac{\pi}{3}) \leq \Pr(\theta_N < \frac{\pi}{3})^m \leq (1 - \delta^N)^m,$$

*which goes to 0 as  $m \rightarrow \infty$ .*

*Proof.* It follows immediately from Lemma 3.6 that in  $N$  steps we achieve  $\Pr(\theta_{i+N} - \theta_i \geq N\varepsilon) \geq \delta^N$ , or put differently, setting  $N = \lceil \frac{\pi}{3\varepsilon} \rceil$ , we get

$$\Pr(\theta_N \geq \frac{\pi}{3}) \geq \Pr(\theta_N \geq N\varepsilon) \geq \delta^N = \delta^{\lceil \frac{\pi}{3\varepsilon} \rceil} > 0.$$

This proves the first statement. The second statement follows from the Markovianity of the process.  $\square$

In order to generalize Corollary 3.7 to the desired setting we will treat the effects of the Riemannian metric and the higher order terms of  $f$  as a perturbation on the algorithm. We start with the following general perturbation result.

**Lemma 3.8.** *Let  $G$  be a linear vector field on  $\mathbb{R}^n$  and let  $\eta > 0$  be given. Moreover let  $P$  be a (not necessarily linear) vector field on  $\mathbb{R}^n$  satisfying  $\|P(\mathbf{x})\| \leq C\|\mathbf{x}\|^2$  for some  $C > 0$ . Then it holds that*

$$\|\mathbf{x} - \eta G\mathbf{x} - (\mathbf{y} - \eta(G + P)\mathbf{y})\| \leq \|\mathbb{1} + \eta G\| \|\mathbf{x} - \mathbf{y}\| + C\eta \|\mathbf{y}\|^2,$$

*where  $\|\mathbb{1} + \eta G\|$  denotes the operator norm. Hence after  $n$  steps, if the states remain in an  $R$ -ball about the origin,*

$$\|\mathbf{x}_{i+n} - \mathbf{y}_{i+n}\| \leq \|\mathbb{1} + \eta G\|^n \left( \|\mathbf{x}_{i+n} - \mathbf{y}_{i+n}\| + \frac{CR^2}{\|\mathbb{1} + \eta G\| - 1} \right).$$

*Proof.* The first inequality follows from the assumptions using the triangle inequality:

$$\begin{aligned}\|\mathbf{x} - \eta G\mathbf{x} - (\mathbf{y} - \eta(G + P)\mathbf{y})\| &= \|(\mathbf{1} + \eta G)(\mathbf{x} - \mathbf{y}) + \eta P(\mathbf{y})\| \\ &\leq \|\mathbf{1} + \eta G\|\|\mathbf{x} - \mathbf{y}\| + C\eta\|\mathbf{y}\|^2.\end{aligned}$$

Now using the assumption that  $\|\mathbf{y}\| \leq R$ , and by iterating this result for  $n$  steps, we find that

$$\begin{aligned}\|\mathbf{x}_{i+n} - \mathbf{y}_{i+n}\| &\leq \|\mathbf{1} + \eta G\|^n \|\mathbf{x}_{i+n} - \mathbf{y}_{i+n}\| + (\|\mathbf{1} + \eta G\|^{n-1} + \dots + 1)CR^2 \\ &\leq \|\mathbf{1} + \eta G\|^n \left( \|\mathbf{x}_{i+n} - \mathbf{y}_{i+n}\| + \frac{CR^2}{\|\mathbf{1} + \eta G\| - 1} \right).\end{aligned}$$

This concludes the proof.  $\square$

In our case, we can always choose coordinates in which the problem locally looks like the setting of Lemma 3.6 with a perturbation as in Lemma 3.8.

**Lemma 3.9.** *Let  $(M, g)$  be a Riemannian manifold and let  $f$  be a Morse–Bott function on  $M$ . If  $\mathbf{x} \in M$  is a critical point of  $f$ , then there exists a chart  $\sigma : U \rightarrow \mathbb{R}^n$  about  $\mathbf{x}$  such that, with  $\mathbf{x} = (x_1, \dots, x_p, y_1, \dots, y_q, z_1, \dots, z_{n-p-q})$*

$$\begin{aligned}\sigma(\mathbf{x}) &= 0, \\ f \circ \sigma^{-1}(\mathbf{x}) &= a_1x_1^2 + \dots + a_px_p^2 - (b_1y_1^2 + \dots + b_qy_q^2) + \mathcal{O}(x^2), \\ g_{ij}(\mathbf{x}) &= \delta_{ij} + \mathcal{O}(x),\end{aligned}$$

where  $\delta_{ij}$  denotes the Kronecker symbol.

*Proof.* Choose coordinates about  $\mathbf{x}$  such that the metric is Euclidean at the  $x$  (e.g. normal coordinates), then use orthogonal transformation to diagonalize the Hessian of  $f$  at  $x$ .  $\square$

Now we can combine the three previous results.

**Lemma 3.10.** *Let  $M$  be a Riemannian manifold and let  $f$  be a Morse–Bott function. For any strict saddle point  $\mathbf{x} \in \text{Crit}(f)$  with value  $f(\mathbf{x}) = c$  there exists  $N > 0$  and a neighborhood  $U$  of  $\mathbf{x}$  such that*

$$\Pr(f(\mathbf{x}_{i+N}) < c \mid \mathbf{x}_i \in U) > \delta.$$

*Proof.* This follows immediately from Corollary 3.7, Lemma 3.8 and Lemma 3.9.  $\square$

**Lemma 3.11.** *Let  $M$  be a Riemannian manifold and let  $f$  be a Morse–Bott function. Further assume that  $f$  has compact sublevel sets and that  $\mathbf{x}_0 \in M$  is not a critical point of  $f$ . Then the probability that  $\mathbf{x}_i$  converges to a critical submanifold of a strict saddle points as  $i \rightarrow \infty$  is zero.*



*Proof.* Consider some critical value  $c$  of  $f$  and let  $C \subset M$  be a connected component of the corresponding critical submanifold made up of strict saddle points, cf. (Nicolaeescu, 2011, Def. 2.41). Note that  $C$  is compact. We will show that the probability that  $\mathbf{x}_i$  converges to  $C$  is zero. Indeed let  $\mathbf{z} \in C$  be arbitrary. Then, by Lemma 3.10, there exists an open set  $U \subset M$  containing  $\mathbf{z}$  such that  $\Pr(f(\mathbf{x}_{i+N}) < c | \mathbf{x}_i \in U) > \delta$  for some  $\delta > 0$  and  $N > 0$ .

Moreover, by compactness we can find a finite collection of such open sets covering  $C$ . Hence it suffices to show that the probability that  $\mathbf{x}_i$  has an accumulation point in  $C \cap U$  is zero. Consider a sequence  $\mathbf{x}_i$  and let  $\mathbf{z} \in C \cap U$  be an accumulation point. Consider two balls  $B_{R_1}(\mathbf{z}), B_{R_2}(\mathbf{z})$  centered on  $\mathbf{z}$  with  $0 < R_2 < R_1$  and both balls contained in  $U$ . Choosing  $R_1$  and  $R_2/R_1$  small enough we can guarantee that  $\mathbf{x}_0 \notin B_{R_1}(\mathbf{z})$  and that any realization needs at least  $N$  steps to traverse the spherical shell  $B_{R_1} \setminus B_{R_2}$ . Now choosing a sequence of strictly decreasing  $R_k$  with  $R_1$  and all  $R_{2k}/R_{2k-1}$  small enough as above we see that the sequence must traverse all shells  $B_{R_{2k-1}} \setminus B_{R_{2k}}$ .

This shows that any sequence with accumulation point in  $C \cap U$  must, infinitely often, spend  $N$  consecutive steps in  $U$ . By Lemma 3.10 the probability that this happens is zero. Here we used the fact that by Markovianity the behaviour of each sequence of  $N$  consecutive steps behaves independently. This concludes the proof.  $\square$

### 3.3 Almost Sure Convergence

The results proven so far guarantee that the algorithm converges almost surely to the set of local minima:

**Proposition 3.12.** *Let  $M$  be a Riemannian manifold and let  $f : M \rightarrow \mathbb{R}$  be an  $\ell$ -smooth Morse–Bott function with compact sublevel sets. Assume that  $\mathbf{x}_0$  is not a critical point. Then for stepsize  $\eta \leq 1/\ell$  the randomized gradient descent algorithm converges almost surely to the set of local minima.*

*Proof.* Since by Lemma 3.4 the function value cannot increase, and since by compactness of sublevel sets the function is lower bounded, the function value must (surely) converge to some value  $f^*$ . By Corollary 3.5,  $f^*$  is almost surely a critical value. By Lemma 3.11 the algorithm almost surely does not converge towards a strict saddle point. Hence we converge almost surely to the set of local minima.  $\square$

In order to prove convergence to a single local minimum, we first need the following lemma.

**Lemma 3.13.** *Let  $\mathcal{E}_i$  be probability distributions with values in the interval  $[0, 1]$  and let  $E_i \sim \mathcal{E}_i$  for  $i \in \mathbb{N}$ . Let  $\varepsilon > 0$ . We assume that there is  $q > 0$  such that*

$$\Pr(E_i \geq \varepsilon | E_1 = e_1, \dots, E_{i-1} = e_{i-1}) \geq q$$

*for all  $i \in \mathbb{N}$  and for all  $e_1, \dots, e_{i-1} \in [0, 1]$ . Then for any  $\alpha \in (0, q \ln \frac{1}{1-\varepsilon})$  it holds that almost surely*

$$\prod_{i=1}^n (1 - E_i) \leq e^{-\alpha n}$$

for  $n$  large enough.

*Proof.* First recall the following basic fact. Consider a sequence of i.i.d. biased coin tosses  $X_i \in \{0, 1\}$  with  $\Pr(X_i = 1) = q$ . By the strong law of large numbers (Jacod and Protter, 2004, Thm. 20.1) the average  $\bar{X}_n = \frac{1}{n} \sum_{i=1}^n X_i$  converges almost surely to the expectation  $q$ . Hence for any  $p \in (0, q)$ , there almost surely exists some  $n_0$  large enough such that  $\bar{X}_n \geq p$  for all  $n > n_0$ .

Let any value  $n$ , and index set  $I = \{i_1, \dots, i_k\} \subseteq \{1, \dots, n\}$  (ordered increasingly) be given. Then

$$\begin{aligned} \Pr(E_i \geq \varepsilon, \forall i \in I) &= \Pr(E_{i_k} \geq \varepsilon \wedge \dots \wedge E_{i_1} \geq \varepsilon) \\ &= \Pr(E_{i_k} \geq \varepsilon \mid E_{i_{k-1}} \geq \varepsilon \wedge \dots \wedge E_{i_1} \geq \varepsilon) \dots \Pr(E_{i_1} \geq \varepsilon) \\ &\geq q^k \\ &= \Pr(X_{i_k} = 1, \dots, X_{i_1} = 1) \end{aligned}$$

and thus we have the following: For all  $p \in (0, q)$ , there almost surely exists some  $n_0$  large enough such that for all  $n > n_0$  it holds that at least  $pn$  of the  $E_i$  are greater than or equal to  $\varepsilon$ . In this case

$$\prod_{i=1}^n (1 - E_i) \leq (1 - \varepsilon)^{np} = e^{-\alpha n},$$

with  $\alpha = p \ln \frac{1}{1-\varepsilon}$ . □

**Theorem 3.14.** *Let  $M$  be a Riemannian manifold and let  $f : M \rightarrow \mathbb{R}$  be an  $\ell$ -smooth Morse–Bott function with  $f$  has compact sublevel sets. Further assume that  $\mathbf{x}_0$  is not a critical point of  $f$ . Then, for stepsize  $\eta \leq 1/\ell$ , the randomly projected gradient descent algorithm converges almost surely to a local minimum.*

*Proof.* The idea is the proof is as follows: first we show that almost surely the distance to the set of local minima decreases exponentially. This then implies that the size of each step decreases exponentially as well, and hence the algorithm converges absolutely to a local minimum.

Proposition 3.12 shows that  $\mathbf{x}_i$  converges almost surely to some connected set of local minima denoted  $C$ . Let  $\mathbf{z} \in C$  be such a local minimum, and let  $H(\mathbf{z})$  denote the Hessian at  $\mathbf{z}$ , and let  $a_{\min}(\mathbf{z})$  denote the smallest non-zero eigenvalue of  $H(\mathbf{z})$ . By compactness and continuity  $a_{\min}(\mathbf{z})$  has a minimum on  $C$ , which we denote  $a_{\min}$ . In a small enough neighborhood of  $\mathbf{z}$ , Lemma 3.9 shows that

$$\begin{aligned} \|\text{grad } f(\mathbf{x})\|^2 &= \sum_j 4a_j(\mathbf{z})^2 (x_j - z_j)^2 + \mathcal{O}(\|\mathbf{x} - \mathbf{z}\|^3) \\ &\geq 4a_{\min}(\mathbf{z})f(\mathbf{x}) + \mathcal{O}(\|\mathbf{x} - \mathbf{z}\|^3) \\ &\geq 2a_{\min}(\mathbf{z})f(\mathbf{x}). \end{aligned}$$

Together with Lemma 3.4 we find

$$f(\mathbf{x}_{i+1}) \leq \left(1 - ((\mathbf{u}_i)_N)^2 \delta 2a_{\min}(\mathbf{z})\right) f(\mathbf{x}_i)$$

where  $\delta = \eta(1 - \frac{\ell\eta}{2})$ .

By Lemma 3.13 this shows that there is some  $\alpha > 0$  such that  $f(\mathbf{x}_i) \leq f(\mathbf{x}_0)e^{-\alpha i}$  almost surely for  $i$  large enough. Again by Lemma 3.4 we have that

$$\|\mathbf{x}_{i+1} - \mathbf{x}_i\| \leq \sqrt{\frac{|f(\mathbf{x}_{i+1}) - f(\mathbf{x}_i)|}{\frac{1}{\eta} - \frac{\ell}{2}}}.$$

This shows that

$$\sum_{i=0}^{\infty} \|\mathbf{x}_{i+1} - \mathbf{x}_i\| \leq \frac{1}{\sqrt{\frac{1}{\eta} - \frac{\ell}{2}}} \sum_{i=0}^{\infty} \sqrt{f(\mathbf{x}_i)} = \sqrt{\frac{f(\mathbf{x}_0)}{\frac{1}{\eta} - \frac{\ell}{2}}} \frac{1}{1 - e^{\alpha/2}} < \infty,$$

and so the total length of the trajectory is finite. Thus  $\mathbf{x}_i$  almost surely converges absolutely to a local minimum of  $f$ .  $\square$

## 4 Quantitative Results in Low Dimensions

The goal of this section is to study the hitting time  $\tau$  of the sublevel set of the critical value. By construction, the stochastic process  $x^{(i)}$  is a Markov chain, since the step  $x^{(i+1)} - x^{(i)}$  depends only on the value of  $x^{(i)}$ . As such, for small enough step size  $\eta$  we can approximate the algorithm by an appropriate Ito stochastic differential equation (SDE).

### 4.1 Two-Dimensional Euclidean Case

In the simplest case we consider the Morse function  $f(x, y) = ax^2 - by^2$  on  $\mathbb{R}^2$  in the Euclidean metric. Due to the scale invariance we can normalize the state after each iteration and so we obtain a discrete-time stochastic process on the unit circle. For small enough stepsize  $0 < \eta \ll 1$  the iteration rule is approximately<sup>5</sup> given by

$$\Delta\phi^i = \phi^{i+1} - \phi^i = \eta \frac{a+b}{2} \sin(2\phi) + u_2 \eta \sqrt{(a \cos(\phi))^2 + (b \sin(\phi))^2} \quad (9)$$

where  $\mathbf{u} = (u_1, u_2)$  is chosen uniformly at random from the unit circle and hence

$$\mathbb{E}[\Delta\phi] = \eta \frac{a+b}{2} \sin(2\phi), \quad \text{Var}(\Delta\phi) = \frac{\eta \sqrt{(a \cos(\phi))^2 + (b \sin(\phi))^2}}{2}$$

---

<sup>5</sup>The formula is obtained by locally approximating the unit circle by its tangent line.

Using (Kloeden and Platen, 1992, Sec. 6.2) we can approximate this process using the stochastic differential equation (SDE)

$$d\Phi_t = \frac{a+b}{2} \sin(2\phi) dt + \frac{\sqrt{\eta((a \cos(\phi))^2 + (b \sin(\phi))^2)}}{2} dW_t \quad (10)$$

For simplicity we consider the simplest case  $a = b = 1$ . Then the limiting SDE reads

$$d\Phi_t = \sin(2\Phi_t) dt + \frac{\sqrt{\eta}}{2} dW_t$$

The approximation is visualized in Figure 3.

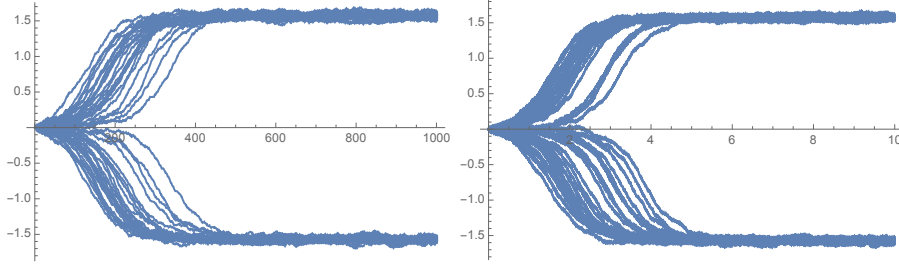


**Fig. 3** We use the constants  $\eta = 0.01$ ,  $T = 10$ ,  $a = b = 1$ . Left: 50 realizations of the stochastic process (9) for  $T/\eta = 1000$  steps. Right: 50 realizations of the stochastic process (10) for time  $T$  and with timestep size  $\Delta t = 0.001$  (simulated using the Euler-Maruyama scheme (Kloeden and Platen, 1992, Sec. 9.1)).

In order to understand how long it takes the algorithm to pass the saddle point we are interested computing in the hitting time

$$\tau = \inf\{t > 0 : \Phi_t = \pm \frac{\pi}{4}\}.$$

Close to the origin, the SDE can be linearized as  $d\Phi_t = 2\Phi_t dt + \frac{\sqrt{\eta}}{2} dW_t$ , which is a mean repelling Ornstein–Uhlenbeck process. Away from the origin, the deterministic part dominates and we can solve the (deterministic) ODE  $\dot{\Phi}_t = \sin(2\Phi_t)$ . First we approximate the hitting time distribution of the repelling Ornstein–Uhlenbeck process.

**Lemma 4.1.** *Let  $X_t$  be the solution of the SDE  $dX_t = \kappa X_t dt + \sigma dW_t$  with  $\kappa, \sigma > 0$  and  $X_0 = 0$ . Setting  $\tilde{\sigma}(t) = \sigma \sqrt{\frac{e^{2\kappa t} - 1}{2\kappa}}$ , it holds that  $X_t \sim \mathcal{N}(0, \tilde{\sigma}(t)^2)$ . If we denote by  $\tau_c$  the hitting time of  $\pm c$  (where  $c > 0$ ), we find the lower bound  $\Pr[\tau_c \leq t] \geq \Pr[|X_t| \geq c] = 1 + \operatorname{erf}\left(\frac{-c}{\tilde{\sigma}(t)\sqrt{2}}\right)$  where  $\operatorname{erf}$  denotes the error function.*

*Proof.* The SDE is linear and hence has the well-known solution

$$X_t = \sigma \int_0^t e^{\kappa(s-t)} dW_s \cong \mathcal{N}(0, \tilde{\sigma}(t)^2)$$

where  $\tilde{\sigma}(t) = \sigma \sqrt{\frac{e^{2\kappa t} - 1}{2\kappa}}$ , see (Kloeden and Platen, 1992, Sec. 4.2 & 4.4). It is clear that if  $|X_t| \geq c$  then  $\tau_c \leq t$ , which implies the last statement.  $\square$

The approximation is very accurate with error smaller than  $\Delta t$  if  $\kappa\Delta t \geq 1$  and  $c \gg \sigma/\sqrt{\kappa}$ , as illustrated in Figure 4.

As in the proof of Lemma 4.1 the solution of the SDE with initial condition  $X_0 = c$  is given by

$$X_t = e^{\kappa t} c + \sigma \int_0^t e^{\kappa(s-t)} dW_s.$$

then

$$e^{\kappa t} c - n\tilde{\sigma}(t) \geq c \implies c \geq n\sigma \sqrt{\frac{e^{2\kappa t} - 1}{2\kappa}} \frac{1}{e^{\kappa t} - 1} \geq \frac{n\sigma}{\sqrt{2\kappa}} \max\left(1, \sqrt{\frac{2}{\kappa t}}\right).$$

Hence for the error in  $\tau_c$  to be small compared to  $\Delta t$ , we need  $c \gg \frac{\sigma}{\sqrt{\kappa}}$  if  $\kappa\Delta t$  is big, and  $c \gg \frac{\sigma}{\kappa\sqrt{\Delta t}}$  if  $\kappa\Delta t$  is small.

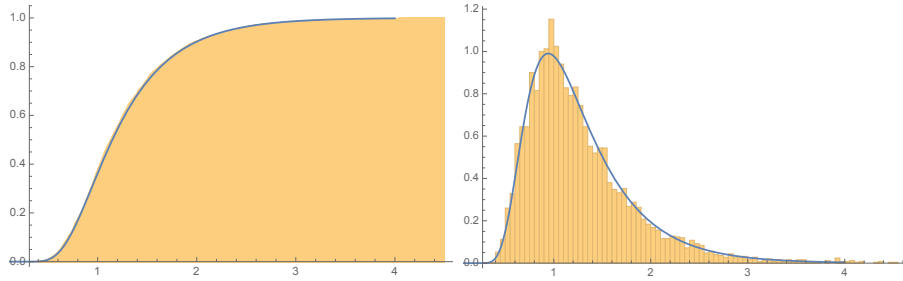


**Fig. 4** We used the constants  $\kappa = 2$ ,  $\sigma = 3$  and  $c = 10$ . Shown are the histograms of the c.d.f. and p.d.f. of  $\tau_c$  computed using timesteps of size 0.001 (orange) and the lower bound for the c.d.f. and the resulting p.d.f. obtained in Lemma 4.1 (blue).

Now if we choose  $c$  small enough that the linearization of  $\sin$  is accurate but large enough that the approximation of Lemma 4.1 is good (which is always possible if  $\eta$  is small enough), then we can approximate  $\tau$  as follows.

We fix some value  $c$  and note that the ODE  $\dot{\phi}_t = \sin(2\phi_t)$  with initial condition  $\phi_0 = c$  has the solution  $\phi_t = \arctan(e^{2t} \tan(c))$ , and hence the hitting time of  $\pi/4$  is  $\tilde{\tau}_c = -\frac{1}{2} \ln(\tan(c))$ . Hence we have approximately  $\tau \simeq \tau_c + \tilde{\tau}_c$ . This is illustrated in Figure 5 for realistic values.

## 5 Ground State Optimization

In quantum information science an important task relates to finding the eigenstate (‘ground state’) and the smallest eigenvalue (‘ground-state energy’) of a Hermitian operator  $A$  that describes the energy of the system (i.e. the Hamiltonian). For this setting, we leave the general notation  $f : M \rightarrow \mathbb{R}$  above and specialise to the cost

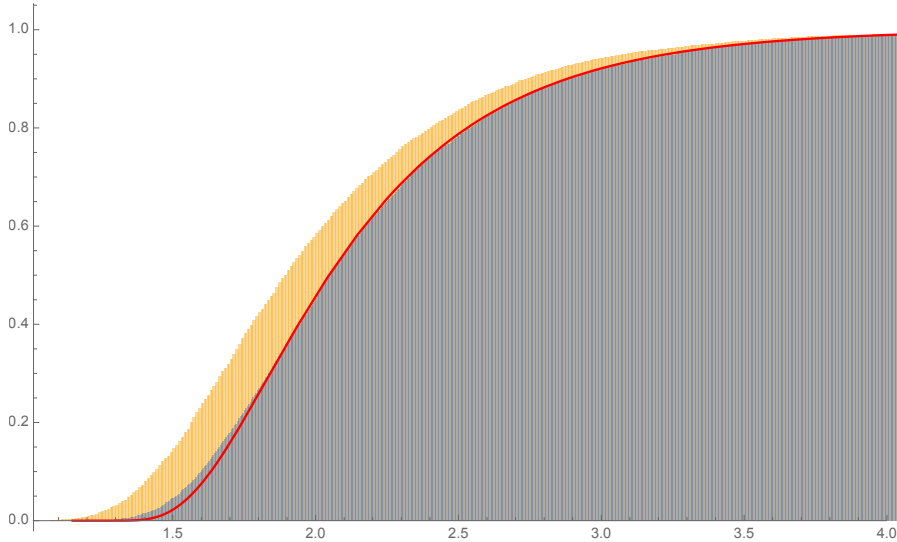


**Fig. 5** Using  $\eta = 0.01$  we plot the c.d.f. of the hitting time  $\tau$  of  $\frac{\pi}{4}$ . In orange for the difference equation, in blue for the stochastic differential equation ( $\Delta t = 0.001$ ), and in red for the analytic approximation.

function over the unitary group (or orbit)  $J : U \rightarrow \mathbb{R}$  we aim to minimize. For finding the smallest expectation value of  $A$  w.r.t. the state  $\rho$ , the cost function is given by

$$J(U) := \text{tr}(AU\rho U^*) = \langle A, \text{Ad}_U(\rho) \rangle, \quad (11)$$

where  $\rho \in \text{pos}_1(n)$  is the initial state of the system and  $U$  is a unitary transformation that describes a quantum circuit (writing  $U^*$  for the complex conjugate transpose).

By choosing an appropriate eigenbasis of  $A$  we may assume that  $A$  is diagonal with eigenvalues in non-increasing order. The function we want to optimize is of the form of Eqn. (11). Many properties of this function can be found in [Duistermaat et al \(1983\)](#) in the more general setting of semisimple Lie groups. We recall the relevant properties here, adapted to our setting:

**Proposition 5.1.** *Assume that  $\rho$  and  $A$  are diagonal<sup>6</sup>. Then the following holds.*

- (i)  *$U$  is a critical point of  $f$  if and only if  $[A, \text{Ad}_U(\rho)] = 0$ . Hence the critical set of  $f$  is equal to*

$$\text{SU}(n)_A \mathcal{S}_n \text{SU}(n)_\rho,$$

*where  $\mathcal{S}_n$  is the set of  $n$  by  $n$  permutation matrices. In particular it is a disjoint union of finitely many compact connected submanifolds.*

- (ii) *The Hessian at a critical point  $U$  is given by*

$$\frac{d^2}{dt^2} \langle A, \text{Ad}_{e^{itH}}(\rho) \rangle = \sum_{i>j} 2(a_i - a_j)(\rho_i - \rho_j) |\langle i | \text{Ad}_U(H) | j \rangle|^2,$$

<sup>6</sup>This amounts to a shift in the function  $f$  and an appropriate choice of basis.

and in particular  $f$  is Morse–Bott.<sup>7</sup>

(iii) There is only one local minimal (resp. maximal) value.

*Proof.* (i): See Lemma 1.1 and Propositions 1.2 and 1.3 of [Duistermaat et al \(1983\)](#).

(ii): See Proposition 1.4 and Corollary 1.5 of [Duistermaat et al \(1983\)](#). (iii): See Remark 1.6 of [Duistermaat et al \(1983\)](#).  $\square$

**Definition 2.** [Gross et al \(2007\)](#)[Thm. 3] A unitary representation  $\pi : G \rightarrow U(n)$ ,  $g \mapsto \pi(g) =: U_g$  a finite group  $G$  is called a unitary  $t$ -design with  $t \in \mathbb{N}_0$  if one of the following equivalent conditions is satisfied:

(a) For all polynomials  $p \in \mathbb{C}_t[Z, \bar{Z}]$  one has the equality

$$\frac{1}{|G|} \sum_{g \in G} p(U_g, \bar{U}_g) = \int_{U(n)} p(U, \bar{U}) dU,$$

where  $\mathbb{C}_t[Z, \bar{Z}]$  denotes the set of all polynomials in  $Z := (z_{ij})_{i,j=1,\dots,n}$  and  $\bar{Z} := (\bar{z}_{ij})_{i,j=1,\dots,n}$ , which are  $t$  homogeneous in  $Z$  and  $\bar{Z}$ , i.e.<sup>8</sup> with  $p(\lambda Z, \mu \bar{Z}) = \lambda^t \mu^t p(Z, \bar{Z})$ .

(b) For all  $H \in \mathbb{C}^{n^t \times n^t}$  one has the equality

$$\frac{1}{|G|} \sum_{g \in G} (U_g \otimes \cdots \otimes U_g) H (U_g \otimes \cdots \otimes U_g)^* = \int_{U(n)} (U \otimes \cdots \otimes U) H (U \otimes \cdots \otimes U)^* dU.$$

(c) One has the equality

$$\frac{1}{|G|} \sum_{g \in G} (U_g \otimes \cdots \otimes U_g) \otimes (\bar{U}_g \otimes \cdots \otimes \bar{U}_g) = \int_{U(n)} (U \otimes \cdots \otimes U) \otimes (\bar{U} \otimes \cdots \otimes \bar{U}) dU.$$

For  $t = 2$  one has the further equivalence

(d) The tensor square representation  $\pi \otimes \pi : G \rightarrow U(n) \otimes U(n)$ ,  $g \mapsto U_g \otimes U_g$  acting on  $\mathbb{C}^n \otimes \mathbb{C}^n$  has exactly two irreducible components, namely  $\text{Sym}(\mathbb{C}^n \otimes \mathbb{C}^n)$  and  $\text{Alt}(\mathbb{C}^n \otimes \mathbb{C}^n) := \mathbb{C}^n \wedge \mathbb{C}^n$ .

**Remark 5.2.** A more general notion of  $t$ -designs [Dankert \(2006\)](#); [Dankert et al \(2009\)](#) (see also [Gross et al \(2007\)](#)) allows any finite subset of  $U(n)$  which satisfies (a), (b) or, equivalently, (c). However, since almost all known examples are constructed via group representations, we focus here on this restricted approach which is sometimes called group design. Moreover, the reader should note the following facts: (i) One can assume without loss of generality that  $\pi$  is faithful (i.e., one-to-one) because it is straightforward to show that  $[g] \mapsto \pi(g)$ ,  $[g] \in G/\ker \pi$  yields a  $t$ -design whenever  $\pi$  is a  $t$ -design. (ii) Every  $t$ -design is also  $t'$ -design for  $t' \leq t$ . This follows readily from condition (b) by choosing  $H$  of the form  $H' \otimes I_n \otimes \cdots \otimes I_n$ .

<sup>7</sup>Note that the function  $f$  is never Morse, since the maximal torus in  $SU(n)$  stabilizes  $A$  and  $\rho$ .

<sup>8</sup>This is equivalent to  $p(\lambda Z, \bar{\lambda} \bar{Z}) = |\lambda|^{2t} p(Z, \bar{Z})$ .

**Lemma 5.3.** *Let  $\pi : G \rightarrow U(n)$  be any unitary representation. Then  $\pi$  yields a 2-design in the sense of Def. 2 if and only if  $\pi$  acts irreducibly on  $\mathfrak{isu}(n)$  via conjugation, i.e. the representation  $\hat{\pi} : G \rightarrow U(\mathfrak{isu}(n))$ ,  $\pi(g)H := U_g H U_g^*$  is irreducible.*

*Proof.* First,  $\hat{\pi}$  obviously “extends” to  $\tilde{\pi} : G \rightarrow U(\mathbb{C}^{n \times n})$ ,  $\tilde{\pi}(g)A := U_g A U_g^{-1}$ . Then a straightforward computation shows that the representations  $\tilde{\pi}$  and  $g \mapsto U_g \otimes \bar{U}_g$  are equivalent and thus for simplicity we will use the same symbol for both representations. Next, we investigate the commutant of the representations  $U_g \otimes \bar{U}_g$  and  $U_g \otimes U_g$  in  $\mathbb{C}^{n \times n} \otimes \mathbb{C}^{n \times n} \cong \mathbb{C}^{n^2 \times n^2}$ , i.e. we are interested in the solutions  $Z$  of

$$(U_g \otimes \bar{U}_g)Z = Z(U_g \otimes \bar{U}_g) \quad \text{for all } g \in G \quad (12)$$

and

$$(U_g \otimes U_g)Z = Z(U_g \otimes U_g) \quad \text{for all } g \in G, \quad (13)$$

respectively. Eq. (12) and (13) are equivalent to  $Ad_{U_g \otimes \bar{U}_g}(Z) = Z$  and  $Ad_{U_g \otimes U_g}(Z) = Z$ , respectively. Finally, a tedious but straightforward computation shows that the partial transposed operator  $\Phi : \mathbb{C}^{n \times n} \otimes \mathbb{C}^{n \times n} \rightarrow \mathbb{C}^{n \times n} \otimes \mathbb{C}^{n \times n}$ ,  $A \otimes B \mapsto A \otimes B^T$  yield an intertwining map for  $Ad_{U_g \otimes \bar{U}_g}$  and  $Ad_{U_g \otimes U_g}$ , i.e.

$$Ad_{U_g \otimes \bar{U}_g} \circ \Phi = \Phi \circ Ad_{U_g \otimes U_g}.$$

This implies  $\Phi$  maps the commutator of  $\tilde{\pi}$  to the commutator of  $\pi \otimes \pi$  and therefore the dimensions of commutators (and consequently the number of irreducible subspaces) coincide. Thus  $\text{Sym}(\mathbb{C}^n \otimes \mathbb{C}^n)$  and  $\text{Alt}(\mathbb{C}^n \otimes \mathbb{C}^n)$  are the only irreducible subspaces of  $\pi \otimes \pi$  if and only if  $\mathbb{C}I_n$  and  $\mathfrak{sl}_0(n)$  are the only irreducible subspaces to  $\tilde{\pi}$  (or, equivalently,  $\mathfrak{isu}(n)$  is the only irreducible subspace of  $\hat{\pi}$ ).  $\square$

**Remark 5.4.** *Note that the above result does not mean that the tensor square representation  $\pi \otimes \pi$  and  $\tilde{\pi}$  are equivalent and, in fact, they are not—as easy examples demonstrate. A similar result for Lie-algebra representations was elaborated on in Zeier and Zimborás (2015) as follow-up on Zeier and Schulte-Herbrüggen (2011) and in particular on Coquereaux and Zuber (2011).*

**Lemma 5.5.** *Let  $\pi : G \rightarrow U(n)$  be a unitary  $t$ -design with  $t \geq 2$  and let  $H_s \in \mathfrak{isu}(n)$  be a traceless Hermitian matrix. Then any subset of  $\{U_g H_s U_g^*\}_{g \in G}$ , where one element is removed, still spans  $\mathfrak{isu}(n)$ .*

*Proof.* By Lemma 5.3 we know that the  $\hat{\pi}$ -invariant subspace spanned by  $\{U_g H_s U_g^* : g \in G\}$  has to coincide with  $\mathfrak{isu}(n)$  and thus  $\{U_g H_s U_g^* : g \in G\}$  contains a basis of  $\mathfrak{isu}(n)$ . Moreover, by the defining property (b) it is straightforward to see that every 1- and therefore also every 2-design has to act irreducibly on  $\mathbb{C}^n$ . Thus we conclude

$$\sum_{g \in G} U_g H_s U_g^* = 0$$

because the left hand side of the above equation belongs to the commutant of  $\pi$  and has trace zero. Now if there is some  $g_0 \in G$  such that  $\{U_g H_s U_g^* : g \in G, g \neq g_0\}$



does not span  $\text{isu}(n)$ , then  $U_{g_0}H_sU_{g_0}^*$  does not lie in the span of the others, and hence  $\sum_{g \in G} U_g H_s U_g^* \neq 0$ , which contradicts the above.  $\square$

## 6 Conclusion, Discussion, and Outlook

We have analyzed the convergence properties of a recently introduced Haar-randomly projected gradient descent algorithm for cost functions taking the form of a smooth Morse–Bott function (with compact sublevel sets) on a Riemannian manifold. For making it efficient in quantum optimizations, one can approximate the Haar-random projections via unitary 2-designs. For both scenarios we have proven that (i) the respective algorithm *almost surely escapes saddle points* (Lem. 3.11) and (ii) it *almost surely converges to a local minimum* (Thm. 3.14). Moreover we have studied the time required by the algorithm to pass a saddle point in a simple two-dimensional setting (Sec. 4.1). Note that unlike adiabatic ground-state preparation strategies (that rest on first preparing some desired initial state to find the ground state of some target Hamiltonian), our randomized Riemannian gradient flow algorithm does not require knowledge of the initial state, as the algorithm converges for almost all initial points. Moreover, as in the quantum setting for ground state problems the critical points just comprise saddles and global extrema, here our result implies almost sure convergence to the *global minimum*.

However, our approach inherits a key problem already arising without projections: the overall speed of convergence to globally optimal solutions may be slow Magann et al (2023), since it depends on the scaling of the magnitude of the (projected) Riemannian gradient. For Riemannian optimizations over the unitary group, the gradient magnitude converges to its expectation value (being zero), while the variance is inversely proportional to the dimension  $d = 2^n$  McClean et al (2018). Thus the probability for a gradient magnitude larger than the noise level of a quantum computer decays exponentially with the number of qubits  $n$ . Well known as *barren plateaux problem* in quantum optimization McClean et al (2018), such exponentially flat regions constitute a main challenge to all variational quantum algorithms in high dimensions on quantum computers.

The algorithmic steps analyzed here are entirely modular. In view of future applications the (approximate) random projections w.r.t. the Haar measure may well be replaced by selections from other problem-adapted measures without sacrificing the convergence properties. In particular, one may wish to select the measures such that the projections of the gradient do not subside in numerical noise prematurely and thus circumvent the notorious barren-plateaux problem. Moreover, one may consider random projections into subspaces by techniques of compressed sensing and shadow tomography to better approximate the full gradient flow. Likewise, approximations with tensor-network methods (such as, e.g., Vanderstraeten et al (2016, 2019)) may be envisaged as long as one remains on a Riemannian manifold. Needless to say the techniques presented here lend themselves to be taken over to higher-order quasi Newton methods (like L-BFGS) also on quantum computers.

Thus we anticipate that the convergence guaranteed for (randomized) Riemannian gradient flows w.r.t. Morse–Bott type smooth cost functions will encourage wide application in and beyond quantum optimization.

## Acknowledgements

E.M. and T.S.H. are supported by the *Munich Center for Quantum Science and Technology* (MCQST) and the *Munich Quantum Valley* (MQV) with funds from the Agenda Bayern Plus. C.A. acknowledges support from the National Science Foundation (Grant No. 2231328) and Knowledge Enterprise at Arizona State University.

## Appendix

### A Some Technical Results

The probability distributions of  $u_N$  and  $u_N^2$  are important for understanding the behaviour of the algorithm. Fortunately they can be described quite easily using the beta distribution. Recall that the p.d.f of the beta distribution with parameters  $a, b$  is given by  $f(x) = \text{const} \cdot x^{a-1}(1-x)^{b-1}$ .

**Lemma A.1.** *If  $u \sim \mathcal{U}(S^{N-1})$  and  $u_N$  is the last coordinate, then*

$$u_N \sim \mathcal{B}_N := 2\text{Beta}\left(\frac{N-1}{2}, \frac{N-1}{2}\right) - 1, \quad u_N^2 \sim \mathcal{B}_N^2 := \text{Beta}\left(\frac{1}{2}, \frac{N-1}{2}\right)$$

where  $\text{Beta}(a, b)$  denotes the beta distribution, and hence

$$\mathbb{E}[u_N^2] = \frac{1}{N}, \quad \text{Var}(u_N^2) = \frac{2(N-1)}{N^2(N+2)}.$$

*Proof.* Let  $Z_1, \dots, Z_N$  be i.i.d standard normals. Then a uniformly random unit vector can be obtained by normalizing the vector  $(Z_1, \dots, Z_N) \in \mathbb{R}^N$ . Considering the last coordinate we see that  $u_N \stackrel{D}{=} Z_1 / \sqrt{Z_1^2 + \dots + Z_N^2}$ . Hence using a well-known relation between the beta and  $\chi^2$  (chi-squared) distributions<sup>9</sup> we find

$$u_N^2 \stackrel{d}{=} \frac{Z_1^2}{Z_1^2 + (Z_2^2 + \dots + Z_N^2)} \sim \text{Beta}\left(\frac{1}{2}, \frac{N-1}{2}\right)$$

Since  $u_N$  is symmetrically distributed around 0, it is easy to compute its p.d.f. starting from that of  $u_N^2$ , and one obtains the form given above. The expectation and variance of  $u_N^2$  follow easily from the formula for the moments of a beta distributed variable  $X \sim \text{Beta}(a, b)$ :

$$\mathbb{E}[X^k] = \prod_{r=0}^{k-1} \frac{a+r}{a+b+r}.$$

---

<sup>9</sup>If  $X \sim \chi_a^2$  and  $Y \sim \chi_b^2$  are independent, then  $\frac{X}{X+Y} \sim \text{Beta}\left(\frac{a}{2}, \frac{b}{2}\right)$ , see (Balakrishnan and Nevzorov, 2003, Sec. 20.8 and 24.4).

This concludes the proof.  $\square$

**Lemma A.2.** For  $N \geq 5$  it holds that

$$d_K(\sqrt{N}\mathcal{B}_N, \mathcal{N}(0, 1)) \leq \frac{1}{N}$$

where  $d_K$  denotes the Kolmogorov distance (the supremum distance between the cumulative distribution functions). This shows that  $u_N^2$  is almost distributed according to the distribution  $1/N\chi_1^2$ , more precisely

$$d_K(N(\mathcal{B}_N)^2, \chi_1^2) \leq \frac{2}{N}.$$

If  $\Phi$  denotes the cumulative distribution function of a standard normal distribution, then for any  $k \geq 0$  it holds that

$$\Pr\left(u_N^2 \geq \frac{1}{k^2 N}\right) \geq 2\left(1 - \Phi\left(\frac{1}{k}\right) - \frac{1}{N}\right).$$

*Proof.* The first inequality follows from (Pinelis and Molzon, 2016, p. 20) and (Pinelis, 2015, Thm. 1.2). It is easy to see that taking the square of both distributions at most doubles the Kolmogorov distance, and this yields the second inequality. Finally we compute

$$\Pr\left(u_N^2 \geq \frac{1}{k^2 N}\right) = 2\left(1 - \Pr\left(u_N \leq \frac{1}{k\sqrt{N}}\right)\right) \geq 2\left(1 - \Phi\left(\frac{1}{k}\right) - \frac{1}{N}\right),$$

proving the third inequality.  $\square$

**Lemma A.3.** Let  $M$  be a compact manifold and let  $\{v_j\}_{j=1}^k$  be a set of continuous vector fields on  $M$  which span the tangent space at every point. Now let any vector field  $v$  on  $M$  be given. Then it holds that there is some  $\varepsilon > 0$  such that

$$\min_{x \in M} \max_i \langle v_i, v \rangle^2 = \varepsilon.$$

*Proof.* The functions  $\langle v_j, v \rangle^2$  defined on  $M$  are smooth and non-negative. Hence their maximum over  $j$  is still a continuous non-negative function on  $M$ . Since the  $v_j$  span each tangent space, this function is even strictly positive, and by compactness of  $M$ , there is a positive global minimum.  $\square$

## References

- Absil PA, Mahony R, Sepulchre R (2008) Optimization Algorithms on Matrix Manifolds. Princeton University Press, Princeton
- Ambrosio L, Brué E, Semola D, et al (2021) Lectures on Optimal Transport, vol 130. Springer

- Balakrishnan N, Nevzorov V (2003) A Primer on Statistical Distributions. Wiley & Sons, New Jersey
- Banyaga A, Hurtubise D (2004) A Proof of the Morse–Bott Lemma. *Expp Math* 22:365–373
- Banyaga A, Hurtubise D (2010) Morse–Bott Homology. *Trans Am Math Soc* 362:3997–4043
- Batselier K, Yu W, Daniel L, et al (2018) Computing Low-Rank Approximations of Large-Scale Matrices with the Tensor Network Randomized SVD. *SIAM J Matrix Anal Appl* 39:1221–1244
- Berger M (2003) A Panoramic View of Riemannian Geometry. Springer, Berlin Heidelberg
- Bharti K, Cervera-Lierta A, Kyaw TH, et al (2022) Noisy Intermediate-Scale Quantum Algorithms. *Rev Mod Phys* 94:015004
- Biamonte J, Wittek P, Pancotti N, et al (2017) Quantum Machine Learning. *Nature* 549(7671):195–202
- Bittel L, Kliesch M (2021) Training Variational Quantum Algorithms Is NP-Hard. *Phys Rev Lett* 127:120502
- Bloch A (ed) (1994) Hamiltonian and Gradient Flows, Algorithms and Control. Fields Institute Communications, American Mathematical Society, Providence
- Brockett R (1988) Dynamical Systems That Sort Lists, Diagonalise Matrices, and Solve Linear Programming Problems. In: *Proc. IEEE Decision Control, 1988, Austin, Texas*, pp 779–803, reproduced in: *Lin. Alg. Appl.*, 146 (1991), 79–91
- Brockett R (1989) Least-Squares Matching Problems. *Lin Alg Appl* 122-4:761–777
- Brockett R (1993) Differential Geometry and the Design of Gradient Algorithms. *Proc Symp Pure Math* 54:69–91
- Cerezo M, Arrasmith A, Babbush R, et al (2021) Variational Quantum Algorithms. *Nature Rev Phys* 3:625–644
- Chu MT, Driessel KR (1990) The Projected Gradient Method for Least-Squares Matrix Approximations with Spectral Constraints. *SIAM J Numer Anal* 27:1050–1060
- Coquereaux R, Zuber J (2011) On Sums of Tensor and Fusion Multiplicities. *J Phys A* 44:295208

- Curry HB (1944) The Method of Steepest Descent for Non-linear Minimization Problems. *Q Appl Math* 2:258–261
- Curtef O, Dirr G, Helmke U (2012) Riemannian Optimization on Tensor Products of Grassmann Manifolds: Applications to Generalized Rayleigh-Quotients. *SIAM J Matrix Anal Appl* 33:210 – 234. <https://doi.org/https://doi.org/10.1137/100792032>
- Dankert C (2006) Efficient Simulation of Random Quantum States and Operators, URL <https://doi.org/10.48550/arXiv.quant-ph/0512217>, MSc Thesis Univ. Waterloo
- Dankert C, Cleve R, Emerson J, et al (2009) Exact and Approximate Unitary 2-Designs and Their Application to Fidelity Estimation. *Phys Rev A* 80:012304
- Duistermaat JJ, Kolk JAC, Varadarajan VS (1983) Functions, Flows and Oscillatory Integrals on Flag Manifolds and Conjugacy Classes in Real Semisimple Lie Groups. *Compositio Math* 49:309–398
- Farhi E, Goldstone J, Gutmann S (2014) A Quantum Approximate Optimization Algorithm, URL <https://doi.org/10.48550/arXiv.1411.4028>
- Fetecau R, Patacchini F (2022) Well-Posedness of an Interaction Model in Riemannian Manifolds. *Commun Pure Appl Anal* 21:3559–3585
- Grimsley HR, Economou SE, Barnes E, et al (2019) An Adaptive Variational Algorithm for Exact Molecular Simulations on a Quantum Computer. *Nature Comm* 10:3007
- Gross D, Audenaert K, Eisert J (2007) Evenly Distributed Unitaries: On the Structure of Unitary Designs. *J Math Phys* 48:052104
- Gustafson K, Rao D (1997) Numerical Range: The Field of Values of Linear Operators and Matrices. Springer, New York
- Helmke U, Moore J (1994) Optimisation and Dynamical Systems. Springer, Berlin
- Irwin MC (1980) Smooth Dynamical Systems. Academic Press, New York
- Jacod J, Protter P (2004) Probability Essentials, 2nd edn. Springer, Berlin Heidelberg
- Kehrein S (2006) The Flow-Equation Approach to Many-Particle Systems, Springer Tracts in Physics, vol 217. Springer, Berlin
- Kloeden PE, Platen E (1992) Numerical Solution of Stochastic Differential Equations. Stochastic Modelling and Applied Probability, Springer, Heidelberg
- Lageman C (2007) Convergence of Gradient-Like Dynamical Systems and Optimization Algorithms. PhD Thesis, Universität Würzburg

- de Lathauwer L, de Moor B, Vandewalle J (2000) On the Best Rank-1 and Rank- $(R_1, R_2, \dots, R_n)$  Approximation of Higher-Order Tensors. *SIAM J Matrix Anal Appl* 21:1324–1342
- Lee J (2013) *Introduction to Smooth Manifolds*, 2nd edn. Springer, New York
- Lee J, Magann AB, Rabitz HA, et al (2021) Progress toward Favorable Landscapes in Quantum Combinatorial Optimization. *Phys Rev A* 104:032401
- Lee JD, Panageas I, Piliouras G, et al (2019) First-Order Methods Almost Always Avoid Strict Saddle Points. *Math Program* 176:311–337
- Li CK (1994)  $C$ -Numerical Ranges and  $C$ -Numerical Radii. *Lin Multilin Alg* 37:51–82
- Lojasiewicz S (1984) Sur les Trajectoires du Gradient d’une Fonction Analytique. *Seminari di Geometria 1982-1983*. Università di Bologna, Istituto di Geometria, Dipartimento di Matematica
- Luenberger DG, Ye Y (2008) *Linear and Nonlinear Programming*, 3rd edn. Springer, Berlin
- Magann AB, Arenz C, Grace MD, et al (2021) From Pulses to Circuits and Back Again: A Quantum Optimal Control Perspective on Variational Quantum Algorithms. *PRX Quantum* 2:010101
- Magann AB, Rudinger KM, Grace MD, et al (2022) Feedback-Based Quantum Optimization. *Phys Rev Lett* 129:250502
- Magann AB, Economou SE, Arenz C (2023) Randomized Adaptive Quantum State Preparation. *Phys Rev Res* 5:033227
- McClellan JR, Boixo S, Smelyanskiy VN, et al (2018) Barren Plateaux in Quantum Neural Network Training Landscapes. *Nature Commun* 9:4812
- Mielke A (2023) An Introduction to the Analysis of Gradient Systems, URL <https://doi.org/10.48550/arXiv.2306.05026>
- Nesterov Y (2004) *Introductory Lectures on Convex Optimization*. Applied Optimization, Springer, New York
- Neuberger J (2010) *Sobolev Gradients and Differential Equations*. Lecture Notes in Mathematics, Springer, Berlin, <https://doi.org/10.1007/978-3-642-04041-2>
- Nicolaescu L (2011) *An Invitation to Morse Theory*, 2nd edn. Springer, New York
- Peruzzo A, McClellan J, Shadbolt P, et al (2014) A Variational Eigenvalue Solver on a Photonic Quantum Processor. *Nature Commun* 5:4213

- Pinelis I (2015) Exact Bounds on the Closeness Between the Student and Standard Normal Distributions. *ESAIM: Prob Statistics* 19:24–27
- Pinelis I, Molzon R (2016) Optimal-Order Bounds on the Rate of Convergence to Normality in the Multivariate Delta Method. *Electron J Statist* 10:1001–1063
- Ruder S (2016) An Overview of Gradient Descent Optimization Algorithms, URL <https://doi.org/10.48550/arXiv.1609.04747>
- Savas B, Lim LH (2010) Quasi-Newton Methods on Grassmannians and Multilinear Approximations of Tensors. *SIAM J Scientific Computing* 32:3352 – 3393. <https://doi.org/https://doi.org/10.1137/090763172>
- Schulte-Herbrüggen T, Glaser S, Dirr G, et al (2010) Gradient Flows for Optimisation in Quantum Information and Quantum Dynamics: Foundations and Applications. *Rev Math Phys* 22:597–667
- Smith ST (1993) Geometric Optimization Methods for Adaptive Filtering. PhD Thesis, Harvard University, Cambridge MA
- Smith ST (1994) Hamiltonian and Gradient Flows, Algorithms and Control, American Mathematical Society, Providence, chap Optimization Techniques on Riemannian Manifolds, pp 113–136. Fields Institute Communications
- Takens F (1971) A Solution. In: Kuiper N (ed) *Manifolds - Amsterdam 1970*. Lecture Notes in Math., 197, Springer, New York, p 231
- Tang HL, Shkolnikov V, Barron GS, et al (2021) Qubit-Adapt-VQE: An Adaptive Algorithm for Constructing Hardware-Efficient Ansätze on a Quantum Processor. *PRX Quantum* 2:020310
- Tilly J, Chen H, Cao S, et al (2022) The Variational Quantum Eigensolver: A Review of Methods and Best Practices. *Phys Reports* 986:1–128
- Vanderstraeten L, Haegeman J, Corboz P, et al (2016) Gradient Methods for Variational Optimization of Projected Entangled-Pair States. *Phys Rev B* 94:155123
- Vanderstraeten L, Haegeman J, Verstraete F (2019) Tangent-Space Methods for Uniform Matrix Product States. *SciPost Phys Lect Notes* 7:1–77
- Wegner F (1994) Flow-Equations for Hamiltonians. *Ann Phys (Leipzig)* 3:77–91
- Wiersema R, Killoran N (2023) Optimizing Quantum Circuits with Riemannian Gradient Flow. *Phys Rev A* 107:062421
- Zeier R, Schulte-Herbrüggen T (2011) Symmetry Principles in Quantum System Theory. *J Math Phys* 52:113510

Zeier R, Zimborás Z (2015) On Squares of Representations of Compact Lie Algebras.  
J Math Phys 56:081702